REACTIVITY OF ETHYLENE OXIDE

IN CONTACT WITH CONTAMINANTS

A Thesis

by

LINH T.T. DINH

Submitted to the Office of Graduate Studies of
Texas A&M University
in partial fulfillment of the requirements for the degree of

MASTER OF SCIENCE

May 2008

Major Subject: Chemical Engineering

REACTIVITY OF ETHYLENE OXIDE

IN CONTACT WITH CONTAMINANTS

A Thesis

by

LINH T.T. DINH

Submitted to the Office of Graduate Studies of
Texas A&M University
in partial fulfillment of the requirements for the degree of

MASTER OF SCIENCE

Approved by:

Chair of Committee, Sam M. Mannan
Committee Members, Debjyoti Banerjee
Rayford Anthony
Head of Department, Michael Pishko

May 2008

Major Subject: Chemical Engineering

ABSTRACT

Reactivity of Ethylene Oxide
in Contact with Contaminants. (May 2008)
Linh T.T. Dinh, B.S., Ho Chi Minh City University of Technology
Chair of Advisory Committee: Dr. Sam M. Mannan

Ethylene oxide (EO) is a very versatile compound with considerable energy in its ring structure. Its reactions proceed mainly via ring opening and are highly exothermic. Under some conditions, it is known to undergo a variety of reactions, such as isomerization, polymerization, hydrolysis, combustion and decomposition

Due to its very reactive characteristic and widely industrial applications, EO has been involved in a number of serious incidents such as Doe Run 1962, Freeport 1974, Deer Park 1988 and Union Carbide Corporation's Seadrift 1991. The impacts can be severe in terms of death and injury to people, damage to physical property and effects on the environment. For instance, the Union Carbide incident in 1991 caused one fatality and extensive damage to the plant with the property damage of up to 80 million dollars.

Contamination has a considerable impact on EO reactivity by accelerating substantially its decomposition and playing a key role on EO incidents.

In this work, the reactivity of EO with contaminants such as KOH, NaOH, NH_4OH, and EDTA is evaluated. Useful information that is critical to the design and operation of safer chemical plant processes was generated such as safe storage temperatures (onset temperature), maximum temperature, maximum pressure, temperature vs. time, heat and pressure generation rates as a function of temperature and time to maximum rate using adiabatic calorimetry. A special arrangement for the filling-up of the cell was constructed due to the gaseous nature and toxicity of EO. A comparison of their thermal behavior is also presented since several contaminants are studied.

ACKNOWLEDGMENTS

It is a pleasure to thank many people who helped me to make this thesis possible.

I would like to express my gratitude to Dr. Mannan for his constant positive reinforcement all through my program. His personal and professional qualities are immensely appreciated. I will be forever indebted to him for teaching me so much.

I would also like to acknowledge Dr. Debjyoti Banerjee and Dr. Rayford Anthony for serving as members of my advisory committee, and for their time, effort and advice given to me.

I would like to thank Dr. Rogers for his help and recommendation with solving numerous problems that I have encountered in the laboratory and for looking at my endless drafts and having the patience to go over them again and again.

I am thankful to Dr. Levin and Dr.Papadaki for insightful comments and thoughts. Your recommendations helped to drive this research work to excellence.

I want to thank my friends in the MKOPSC for their friendship and support as well as for making my graduate years enjoyable and memorable.

Last, but certainly not the least, I would like to express my sincere gratitude to my parents, Ly Dinh and Hoang Nguyen, my aunt, Huong Nguyen, and my brother, Hung Dinh for their support through my struggle to complete this research. I would also like to thank my boyfriend, Viet Pham, for his encouragement, patience and help during this process.

NOMENCLATURE

Symbols	**Definition**
Subscripts	
adj	Adjusted value
c	Sample cell
max	Maximum
meas	Measured value
MR	Maximum rate
o	Refer to the onset temperature of an exotherm reaction
s	Sample
Parameters	
C	Heat capacity
C_c	Heat capacity at constant pressure for the sample cell
C_s	Heat capacity at constant pressure for the sample
dP/dt_{max}	Maximum pressure rate
dT/dt_{max}	Maximum heat rate
m	Mass
P	Pressure
P_{max}	Maximum pressure
t	Time
T	Temperature
T_{max}	Maximum temperature
t_{MR}	Time to maximum rate
T_o	Onset temperature
Φ	Phi-factor

Abbreviations

APTAC	Automatic pressure tracking adiabatic calorimeter
ARIP	Accidental release information program
ARC	Accelerating rate calorimeter
DTBP	Di-tertiary butyl peroxide
DEA	Diethylene glycol
EDTA	Ethylene Diaminetetraacetic acid
EO	Ethylene Oxide
HSEES	Hazardous substances emergence events surveillance
HWS	Heat-wait-search mode
KOH	Potassium hydroxide
MEG	Monoethylene glycol
NaOH	Sodium hydroxide
NH_4OH	Ammonia hydroxide
RSST	Reactive system screening tool
TEA	Triethylene glycol
VSP	Vent Size Package

TABLE OF CONTENTS

Page

CHAPTER Page

LIST OF FIGURES

FIGURE Page

FIGURE Page

LIST OF TABLES

TABLE Page

CHAPTER I

INTRODUCTION

EO is a very versatile compound, storing considerable energy in its ring structure. Its reactions proceed mainly via ring opening and are highly exothermic. Under some conditions, it is known to undergo a variety of reactions, such as isomerization, polymerization, hydrolysis, combustion, and decomposition.

Due to its very reactive characteristic and widely industrial applications, EO has been involved in a number of serious incidents such as Doe Run 1962, Freeport 1974, Deer Park 1988, and Union Carbide Corporation's Seadrift 1991. The impacts may be severe in terms of death and injury to people, damage to physical property, and effects on the environment. For instance, the incident in the Union Carbide in 1991 caused one fatality and extensive damage to the plant with property damage of up to 80 million dollars.

Effect of contamination is a considerable cause of EO incidents. The presence of trace impurities such as alkalis, acids, oxidizers, iron chlorides, iron oxides, and aluminum may reduce the thermal stability of a nominally pure chemical and cause unexpected runaway reactions under normal process conditions. Furthermore, in the real industry, a wide range of processes of industrial applications involving ethylene oxide has the possibility of contamination by KOH, NaOH, NH_4OH, and EDTA. However, little work has been done to study the reactivity of EO with the above contaminants and to provide important thermal parameters, such as the onset temperature, maximum temperature, maximum pressure, maximum heat rate, and maximum pressure rate. Therefore, to fill those gaps, the reactivity of EO contaminated by KOH, NaOH, NH_4OH, and EDTA was measured in this work using adiabatic calorimetry.

This thesis follows the style of the *AIChE Journal.*

Of available adiabatic calorimeters, APTAC has an advantage of low phi-factor and the ability to follow the sample pressure inside the test cell. The data from APTAC tests include the temperature and pressure as a function of time, which is suitable to the requirement of this work. Hence, the APTAC is chosen to conduct all of the tests in this work. The data that will be measured by the APTAC include:

- Important data curves: temperature profile, pressure profile
- Self heat rate and pressurization rate profiles
- Parameters such as the onset temperature, maximum temperature, maximum pressure, self-heat rate at onset temperature, maximum self-heating rate, and maximum pressure rise rate

The data acquired and the shapes of the curves provide information about potential hazards posed by the reactions that occur in the system. It will also be used in the kinetic analysis of a runaway reaction and the design of safety relief valves.

Before embarking on performing experimental research, it is very important to have a thorough understanding of what has been done in the past and thus be able to identify the gaps and research need. Therefore, this report starts with Chapter II including the background on the physical and chemical properties of EO, followed by discussions of EO industrial production and applications, contamination incidents, and previous research involving EO with contaminants.

Then, Chapter III continues with a review of calorimetry. Chapter IV is dedicated to the detailed information about the experimental equipment and methods used in this thesis. The most important part in this work is discussed in Chapter V involving the results and discussions including the reactivity of EO in the presence of contaminants. Chapter VI summarizes the research by stating the conclusions and recommendations for future work.

CHAPTER II

LITERATURE REVIEW

Ethylene oxide (EO), an important industrial chemical, has been involved in many incidents. The EO involving data analyzed by HSEES and ARIP include 300 incidents in the United States from 1987 to 2001 (see Figure 1)[1, 2].

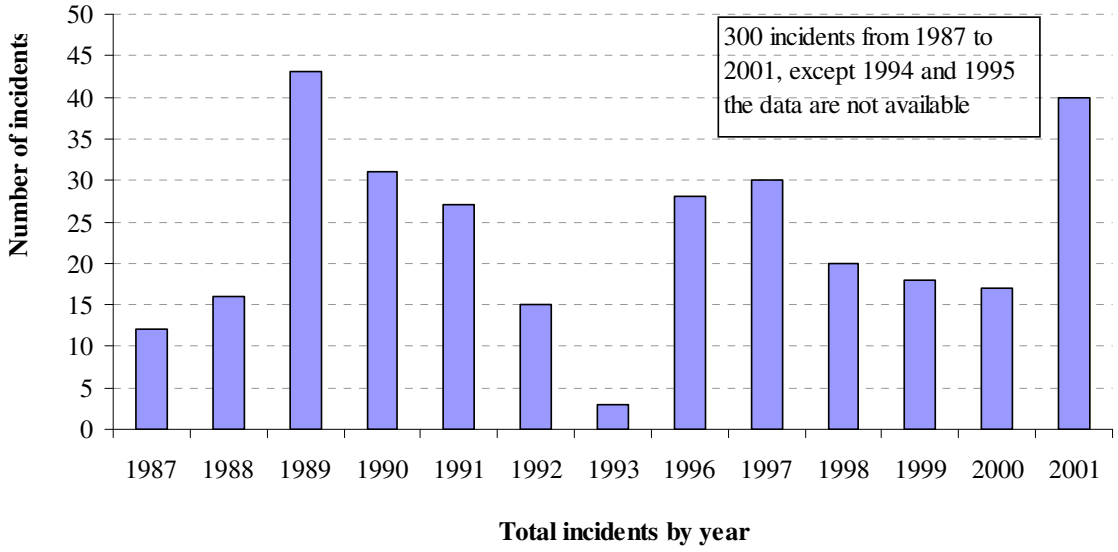

Figure 1 Numbers of incidents from 1987 – 1993 and 1996 – 2001

An average number of EO incidents from 1987 to 1993 was 21 incidents per year while the average number increase to 25.5 incidents per year from 1996 to 2001[1, 2]. Of the 153 EO incidents in the period 1996 and 2001, there were 148 incidents in which EO was released to the environment. From this perspective and because of its toxicity, EO is a dangerous chemical [2].

A large number of factors that contribute to cause the EO incidents include equipment failure, operator error, maintenance, system startup/shutdown, improper mixing, and improper filling/overfill (see Figure 2) [2].

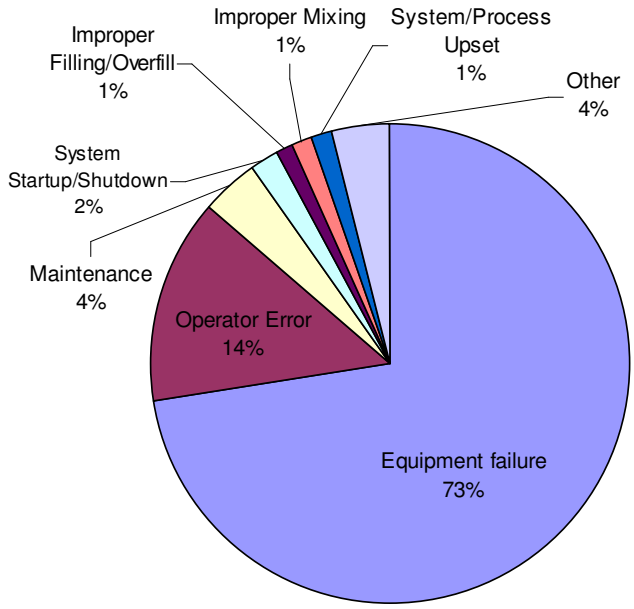

Figure 2 Fractions of occurred incident cause
(Source: Hazardous Substances Emergency Events Surveillance)

The impacts may be severe in terms of death and injury to people, damage to physical property, and effects on the environment. Specifically, one serious incident was the Union Carbide explosion in 1991, which caused one fatality and extensive damage to the plant with the property damage of up to 80 million dollars [3]. According to the investigators, the accident occurred because of a series of coinciding circumstances in which a highly exothermic reaction between EO and iron oxide generated a hot spot with a temperature above the 500^{o}C, EO auto decomposition temperature.

In summary, EO is a significant chemical for which a thorough understanding of its thermal behavior in the different scenarios is needed to prevent or reduce incidents and losses.

In order to develop an understanding of what has been done in the past and thus be able to identify the gaps and research needs, the EO chemical and physical properties and applications, the past contamination incidents of EO, and the previous research involving EO/contaminants will be described in the following sections.

2.1 Properties of ethylene oxide

Ethylene oxide has the molecular formula of H_2COCH_2. It is the simplest of the cyclic ethers and very reactive because of its strained ring [4].

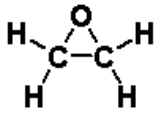

Ethylene oxide is a colorless gas at room temperature and atmospheric pressure. The liquid has a characteristic of ether-like odor [5].

Table 1 Some important physical properties of EO

Property	SI Units
Molecular Weight	44.1
Melting Point	161.46^{o}K
Boiling Point	283.6^{o}K
Flammability Limits	3-100% vol.
Auto ignition temperature	702^{o}K

The vapor density of EO is 1.49 which is approximately 1.5 times heavier than air [5]. Table 1 presents some important physical properties of EO [6].

EO is highly flammable and poses a dangerous fire and explosion risk. Pure EO with a flash point of -18^{o}C can be ignited without air or oxygen. Once ignited, the velocity of EO flash back to the fuel source is 1,800 – 2,400m/sec [5]. High pressure can be generated by the decomposition of EO.

In addition, EO is very a versatile compound, storing considerable energy in its ring structure. Its reactions proceed mainly via ring opening and are highly exothermic. Under appropriate conditions, EO is known to undergo a variety of reactions, such as isomerization, polymerization, hydrolysis, combustion, and decomposition which produce a considerable energy (see Table 2) [7, 8].

Table 2 Heat of reaction of various ethylene oxide reactions at 25^{o}C

Reaction	kJ/kg
Combustion	-27,649
Decomposition	-3,051
Isomerization	-2,621
Polymerization	-2,093
Hydrolysis	-2,081

As a highly reactive compound, EO reacts with many other compounds including: alkalis, acids, oxidizers, chlorides of iron, oxides of iron, and aluminum. Its reactions proceed mainly via ring opening and are highly exothermic. The presence of trace impurities of those chemicals can reduce the thermal stability of a nominally pure chemical and cause unexpected runaway reactions under normal process conditions. Therefore, contamination is considered a main cause of EO incidents.

2.2 Production and application

Ethylene Oxide worldwide production capacity exceeds 11 million tons annually [6]. Today, the capacities of EO production plants are higher, going from 300,000-350,000 tonnes/year to 530,000-590,000 tonnes/year. Around 14-15 new EO/MEG plants are expected to be built including three each in Iran and Saudi Arabia, four in China, and one each in Kuwait, Thailand, Taiwan, and India [9]. This information reveals that ethylene oxide is a major industrial chemical and will continue to be in high demand.

EO is among the top 3% of high-volume chemicals produced in the United States [5], where all ethylene oxide is produced industrially by the direct oxidation of ethylene with air or oxygen in the presence of a silver oxide catalyst. Another commercial production method, reaction of ethylene chlorohydrins with potassium hydroxide or calcium oxide, was phased out by 1980.

Some primary U.S. ethylene oxide manufacturers are BASF Corp, Parsippany, NJ; Dow Chemical USA, Midland, MI ; Eastman Chemical Co, Kingsport, TN; Hoechst Celanese Corp, Somerville, NJ; Occidental Petroleum Corp, Los Angeles, CA; PD Glycol, Beaumont, TX; Shell Chemical Co, Houston, TX; Sun Company Inc (R&M), Philadelphia, PA; Dow Co, Danbury, CT; Texaco Chemical Co, Houston, TX; and Formosa Plastics Corporation U.S.A., Livingston, NJ [10].

Ethylene oxide is most useful as a raw material for ethylene glycol, which is widely used in heat transfer fluids and synthetic fibers. The other chemicals produced from EO are nonionic surfactants (14%, used in industrial applications, detergents, and dishwashing formulations), glycol ethers (6%), ethanolamines (8%) (used in soaps, detergents, and textile chemicals), triethylene glycol (2%), and diethylene glycol (6%). It is also used as a sterilant and fumigant in the health product and medical field.

2.3 Contamination incidents involving EO

Due to its very reactive characteristic and wide industrial applications, EO has been involved in a number of serious incidents resulting in major damage as well as fatalities [3, 7, 8, 11-14].

The fact that EO can react when in contact with numerous other species such as oxides of iron, alkalis, strong acids, oxidizers, chlorines of iron, and aluminum, contamination is considered one of the most significant hazards. Among those contaminants, this work focused on four contaminants including potassium hydroxide, sodium hydroxide, ammonia hydroxide, and ethylene diamine tetraacetic acid due to their high possibilities to contact with EO and their past contamination incidents.

It is true that the above contaminants can contact EO due to their indispensable role in many processes and plants involving EO. As mentioned in the previous section, EO is widely used in the production of many important surfactants and polyglycols by reaction of EO with fatty alcohols, alkyl phenols, or fatty acids [15]. Nevertheless, many of those ethoxylation reactions use an alkali metal hydroxide, more preferably potassium or sodium hydroxide, as a basic catalyst in the ethoxylation. Acid can be used as an acidic catalyst for the formation of polyether. Moreover, acid; specifically, EDTA is also a common acid cleaner for preparing metal surfaces for EO service [6]. For producing mixtures of mono-, di- and triethanolamine, a reaction between aqueous ammonia and EO is performed. The above information reveals a wide range of processes of industrial applications involving ethylene oxide with the possibility of contamination by KOH, NaOH, NH_4OH, and EDTA.

Together with the above positive roles in many industrial applications, the above contaminants may create hazardous situations, resulting in serious incidents if they contact EO for any unintentional reason. The following paragraphs mention some incidents causing by the contaminants chosen for research in this work.

- Alkali hydroxide

An EO polymerization incident brought about by contamination of 90 kg EO-containing cylinder with a small amount of sodium hydroxide was discussed in the AICHE Monograph Series in 1977. The result was a runaway reaction that ended with an explosion after about eight hours [12].

Another ethoxylation reactor caused the explosion during normal operation because the KOH catalyzed a reaction of the EO in the vapor space of the reactor, driving the temperature in localized areas of the reactor head to the decomposition temperature [6, 12].

The third incident happened during ethoxylation of glycerine. Alkali hydroxide was considered as one of the causes of the accident. Local concentrations of alkali arising from the thermal decomposition of potassium soaps presented as an impurity in the sucroglyceride which may have initiated exothermic polymerization of the oxide [12, 13].

- Ammonia

Accidental contamination of a small amount of aqueous ammonia entering the EO storage tank by back-flowing from an ethanolamine unit is believed to have caused a runaway reaction in an EO storage tank (6,500 gallons) at an EO production and derivatives plant at Doe Run in 1968. Violent rupture of the tank led to a devastating vapor cloud explosion. Figure 3 and Figure 4 record the ruins of this incident where EO tanks were no longer visible after the explosion. It damaged in a radius of 500 feet from the blast center, one fatality, three serious injuries, and 18 less serious injuries [6, 14, 15].

The other incident occurred when a railcar of EO was delivered to the wrong plant and the workers at the receiving plant thought the car contained anhydrous ammonia. They attempted to off-load the EO into an anhydrous ammonia tank. The ammonia tank was at a significantly higher pressure than the pressure on the EO railcar. During the attempt to off-load the EO, a check valve leaked and allowed a small amount of ammonia to back

flow into the EO railcar. The explosion caused major damage over a 300-meter radius and broke windows up to 5 km away [6].

Figure 3 Blast center in an incident involving EO

Figure 4 Plant laboratory after EO vapor cloud explosion-300 feet away
Source: Ethylene Oxide User's guide, 2nd Ed

In summary, EO is contaminated in many different ways, such as cleaning processes, failed operation, and human error. Incidents of the EO contamination appear to be unavoidable and very dangerous. Accordingly, it is very important to understand these contamination incidents to enable managing the risks of handling EO.

2.4 Previous research

As has been noted, the hazardous effect of common contaminants such as potassium hydroxide, sodium hydroxide, and aqueous ammonia is a considerable cause of EO incidents. These contamination occurrences, even in an inadvertent manner, under uncontrolled circumstances can pose a significant threat to personnel and can cause equipment damage. However, only a few studies investigated the reactivity of EO in contact with contaminants. Published investigations are for iron oxide, water and sodium hydroxide solution [16-19].

Levin [16] used an APTAC to measure the reactivity of ethylene oxide contaminated with various iron oxides, including γ-Fe_2O_3, α-Fe_2O_3, α-Fe_3O_4, and FeO. The last contaminant (FeO) had no effect on the exothermic decomposition of ethylene oxide. All of these iron oxides, except FeO, exhibited exothermic reactivity below 100^{o}C. The contaminant γ-Fe_2O_3 was found to be the most hazardous one in an aspect of easier exotherm ignition, because the onset temperatures in its presence reduced to as low as room temperature. The relative reactivity was concluded to be in order of γ-Fe_2O_3 > α-Fe_3O_4 > (hydrated) α-Fe_2O_3 > α-Fe_2O_3 >> FeO $\approx$ glass.

The reactions of ethylene oxide-water and ethylene oxide-ethylene glycol were studied by Arthur D. Little, Inc [18]. In this thorough study, experiments on a wide range of water and ethylene glycol concentrations in ethylene oxide were carried out in the ARC and APTAC adiabatic calorimeters. Heats of reaction, physical properties, and vapor-liquid equilibriums, and finally unique fourth-order kinetics of these reactions were reported in detail. Then the author used the measured data to develop reaction models which are

useful for the determination of ethylene oxide storage stability and pressure relief system design under water-contamination scenarios.

Britton [16] investigated the thermal stability of pure and contaminated EO in ARC. Pure EO was found to exhibit the exotherm reaction threshold temperature at 210-220^{o}C in titanium bomb. Experiments of EO in the presence of various contaminants such as water, dimethylamine, rust, insulation materials, and chlorides of Sn, Ti, and Fe were performed using ARC. EO with 10 % wt., 40 % wt., and 90 % wt water exhibited a threshold onset temperature of 150^{o}C, 70^{o}C, and 50^{o}C respectively. In the presence of 2g insulation materials, exothem reactions of 2g EO appeared to start at 70^{o}C for asbestos, 85^{o}C for calcium silicate insulation, 120^{o}C for expanded perlite, and 150^{o}C for mineral wool. The ARC threshold self-heat rate of 0.02^{o}C/min was obtained at 33^{o}C for the scenario of EO contaminated by 1 % wt. dimethylamine.

As for aqueous alkali contaminants, a study of the runaway exothermic polymerization of ethylene oxide by 10 wt% of solutions of NaOH with various concentrations was done using an ARC [19]. The sample consisted of 1.8g ethylene oxide and 0.2 g aqueous NaOH solution. The plots of self-heat rate versus temperature for every scenario were produced. The onset temperatures, corrected adiabatic exotherm, maximum pressure, and heat of polymerization was sufficiently reduced by the contamination to 55.0^{o}C, 439^{o}C, 40.5 bar, 44.6 bar, and 1.06 kJ/g for the lowest concentration of 0.125M and 22.5^{o}C, 415^{o}C, 44.6 bar and 1.0kJ/g for the highest concentration of 1M, respectively.

No research for the contaminants KOH, NH_4OH, or EDTA had been done. It was decided to do research on the reactivity of EO in the presence of KOH, (anhydrous) NaOH, NH_4OH, and EDTA in this work. Although NaOH solution contamination was studied, research on anhydrous NaOH contamination is useful also. Such research will provide insights on the effect of NaOH compound alone, while a study of NaOH solution results the combined effects of NaOH and water. Anhydrous NaOH contamination in EO can occur in practice but no publication on this issue was found.

CHAPTER III

CALORIMETERS

3.1 Introduction

Beginning in the 1950's, the necessity to evaluate the chemical exothermic behavior due to instability, incompatibility, oxidization, flammability, or explosibility became evident. It is believed that 20% of process incidents are caused by lack of thermochemical knowledge [20]. The calorimetry approach is mainly applied for the study of thermal stability and runaway reactions.

Although there are many calorimeters, only the ARC, VSP, and APTAC have been specifically designed to obtain thermokinetic and vapor pressure information during runaway reaction conditions. These calorimeters share the same accelerating rate principles. First, the sample is heated to a reaction initiation temperature. The adiabatic condition is maintained by temperature control so that the temperature of the sample and the sample surroundings are maintained as close as possible. When an exothermic reaction occurs, the thermal energy produced will increase the sample temperature resulting in the increase of the reaction rate and the release of even more energy. The reaction rate will increase further thereafter and lead to a runaway reaction [21].

The accelerating rate calorimeter (ARC) is the first instrument designed to study the temperature and pressure profiles generated during a runaway reaction [22]. The technique of this equipment consists of heating the sample to a reaction initiation temperature. The cell is equipped with a thermocouple mounted externally on the wall. The significant advantage that the ARC offers over other calorimetric techniques is its high-sensitivity exothermic onset detection ability of self-heating down to 0.02^{o}C/min. Nevertheless, there are some drawbacks about the ARC such as the necessary use of thick-walled 10 cc cells, since there is no mechanism to back up the generated sample pressure. This kind of

sample cells absorbs a greater portion (compared with a thin wall cell) of the generated energy and decrease the measured self heat values. Another disadvantage is that the heat of reactions must be estimated since the ARC does not directly measure energy in or out of the sample. Its maximum sample self-heat rate matching is limited to approximately 10^{o}C/min.

The VSP apparatus was developed in 1976. In this equipment, the pressure is generated outside the sample vessel to cancel the pressure difference during the reaction to prevent the cell from rupturing. As a result, the sample cell can withstand larger pressures with larger sample sizes compared to the ARC and thinner sample cell walls. These features have the advantage of low phi-factor data for this equipment.

The APTAC combined the features of the Vent Size Package (VSP) bench-scale apparatus (low phi-factor, large-scale sample mass, and high self-heat rates matching) and the ARC (low exotherm onset detection) into a single instrument. APTAC uses the accelerating rate principle of the ARC, the pressure compensating principle of the VSP, and has an improved heater and software design that minimizes heat losses. The APTAC can match temperature and pressure rise rates of up to 400^{o}C/min and 10,000 psi/min, respectively. Table 3 compares some of the characteristics of the ARC, VSP, and APTAC calorimeters [20].

Table 3 Comparison of calorimeters used to obtain process safety data

	ARC	*VSP*	*APTAC*
Maximum adiabatic matching, ^{o}C/min	10	100	400
Maximum pressure matching, psi/min	-	3,000	10,000
Minimum phi-factor attainable	2	1.05	1.1

One of the APTAC's drawbacks is its expense and time-consuming maintenance in contrast with the ARC's simpler design. So, the number of APTAC apparatus used in the world is limited [22]. They were mainly used only by large chemical companies to generate private internal data. However, as mentioned, the APTAC has more advantages compared to the other calorimeters. Moreover, the MKOPSC possesses one APTAC. For these reason, we decided to use the APTAC in this investigation of EO reactivity in contact with contaminants to provide information that can help to prevent incidents in medium and small sized companies. As the instrument used in this research, the APTAC will be emphasized in a separate section.

3.2 Automatic pressure tracking adiabatic calorimeter (APTAC)

3.2.1 Apparatus

The APTAC is an adiabatic closed-cell reaction calorimeter with a spherical sample vessel supported at the top part of a pressure vessel using a nut and a graphite ferrule. The sample vessel temperature is controlled by four main heaters: bottom, top, side, and tube heaters. These heaters and the reaction vessel are surrounded by insulation and placed in a 500-ml pressure vessel. The sample thermocouple, type N, passes directly into the sample vessel through a fitting on the top heater. Six other-type N thermocouples are used to measure the external surface of the sample vessel wall, the temperature of the nitrogen gas surrounding the sample cell, and each of the other thermocouples measure the temperature of one specific heater. The adiabatic condition is maintained by the temperature control software so that the temperatures of the sample and the nitrogen surrounding the sample are maintained as closely as possible. Figure 5 is an overall view of the APTAC system. A detailed schematic of the APTAC pressure vessel is shown in Figure 6.

In this instrument, pressure is measured by means of a transducer with a 0-2,500 psi range and 0.1% of full scale error. Balancing the pressure outside of the sample cell to

match the internal pressure of the sample cell enables the apparatus to probe sample pressures as high as 2,000 psia without bursting the sample vessel [23].

Figure 5 Overall view of APTAC system

3.2.2 Heat-mode operation

The APTAC has various heating modes such as heat-wait-search, heat-soak-search, heat ramp, and isothermal.

In the heat-soak-search mode, the temperature of the sample is held at an elevated temperature until either an exotherm is detected or a pre-set time limit is exceeded.

For the heat ramp mode, a fixed heating rate is selected, and the temperature and pressure of the sample are monitored until an end temperature is reached. No exotherm detection occurs so that heat is input to the reactor by the heaters even during an exotherm [21, 22]. If the temperature of the sample goes above the programmed temperature

increase, there will be heat losses. This mode of operation is similar to that of the reactive system screening tool (RSST) calorimeter.

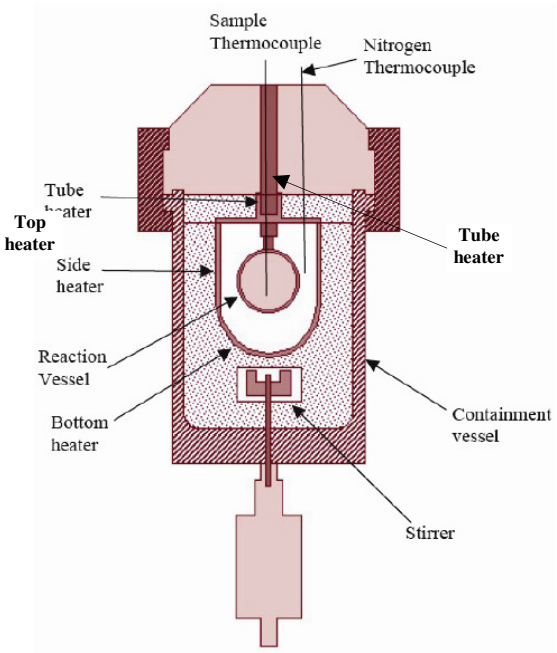

Figure 6 Schematic of the APTAC pressure vessel

In the isothermal mode the sample is heated to a preset temperature and kept at that temperature for a fixed amount of time.

In this research, the focus was on the heat-wait-search (HWS) operation mode. For each experiment, operation was automated and typically started in the HWS mode with an exotherm detection threshold of 0.05 ^{o}C/min. The sample was heated to an initial search temperature and the temperature was allowed to stabilize in 25 minutes. Steps of 10^{o}C were conducted at a rate of 4^{o}C/min. The system changed to search mode to detect an exotherm thereafter (25 minutes more). An exothermic activity was detected when a threshold of self-heating rate of 0.05 ^{o}C/min was exceeded, and the APTAC followed the

reaction adiabatically until the sample was depleted or one of shutdown criteria was satisfied. If no exothermic activity was detected within the search mode, the sample was heated to the next search temperature and the procedure was repeated [24, 25].

Figure 7 shows a typical plot of temperature as a function of time with the search mode of the APTAC below the exothermic region.

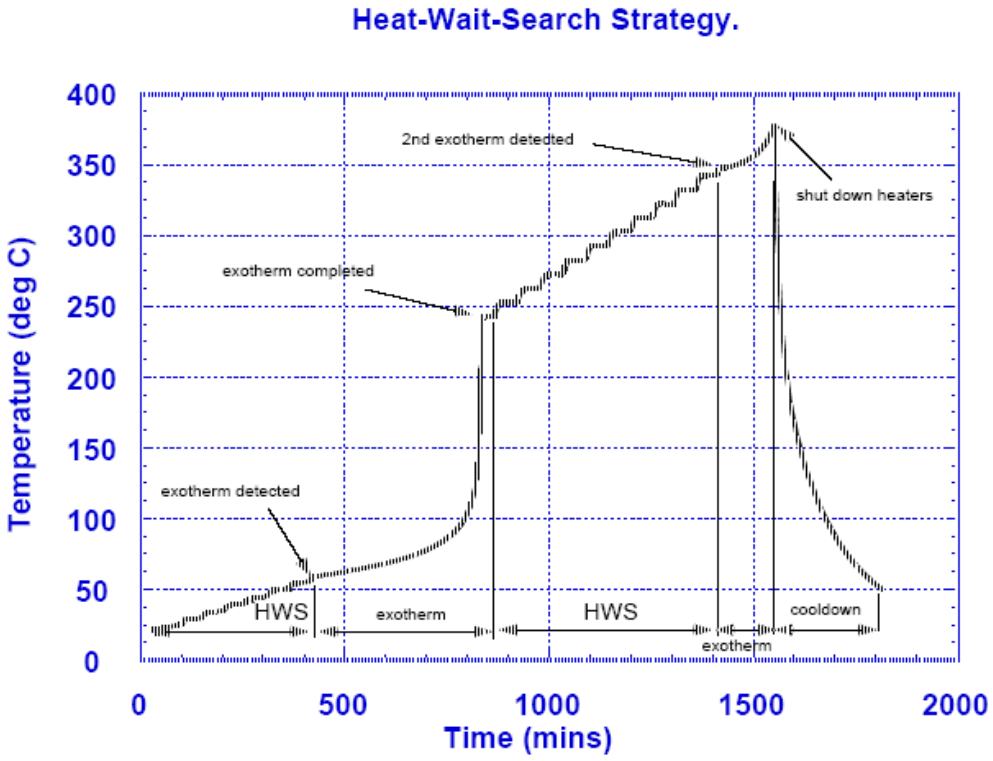

Figure 7 A typical temperature history with the HWS mode in the APTAC
(This figure is extracted from the APTAC manual)

CHAPTER IV

EXPERIMENTAL PROCEDURES AND METHODOLOGY

4.1 Samples

- Aldrich 99+% EO, catalog No 38,761-4, was employed in this thermal analysis. A single pressurized cylinder with 227g EO supplied the EO for all experiments. It was used with no additional purification or treatment processes.

- For some experiments reported in this work, a contaminant of KOH 90 % from Mallinckrodt, catalog number 6984-04 was used. Another contaminant measured was NaOH 99% from Mallinckrodt, catalog number 7708-10.

- Ammonia hydroxide, NH_4OH 30% from Baker, catalog number 9721-01 was used to test its effect on EO.

- For the EDTA contaminant, high purity EDTA 99.999 % from Aldrich catalog number 43,178-8 was used.

- The experiments were conducted under nitrogen environment following evacuation of air from the test cells. High purity compressed nitrogen was used in the APTAC experiments to provide the no-air environment.

EO sample weights ranged from 13.98 to 14.04 g and contaminant weights were 0.1 ± 0.01 g, 0.5 ± 0.02 g, 1.0 ± 0.02 g, while the weight of the titanium cells ranged between 30.43 and 34.56 g.

4.2 Experiment apparatus

All of the data presented in this work were collected with an APTAC calorimeter using the adiabatic mode. A summary of APTAC test conditions is presented in Table 4. The apparatus and operation of APTAC are clearly described in Chapter III.

Table 4 Summary of the APTAC test conditions

Temperature and pressure	Value	Other settings	Value
Start temperature, ^{o}C	20-100	Heat mode: heat-wait-search	
Final temperature, ^{o}C	250	Exotherm threshold, ^{o}C/min	0.05
Temperature increment, ^{o}C	10	Exotherm limit, ^{o}C	300
Cool-down temperature, ^{o}C	50	Heat rate, ^{o}C/ min	4
Temperature shutdown, ^{o}C	500	Heat rate shutdown, ^{o}C/min	400
Pressure shutdown, psia	1,900		
Pressure rate shutdown, psi/min	10,000		

Due to the gaseous nature and toxicity of EO, the normal procedure for external sample loading to the APTAC cell was not applicable and special apparatus was designed. Handling of EO should be done very carefully.

Figure 8 illustrates the special setup used to transfer and measure the weight of the EO sample.

- A small cylinder of 227 g EO (1632 g of total weight) was used to supply EO. Its dimensions were 12 inches height and 2 inches diameter. To stabilize and protect the lecture bottle of EO, a cradle that was wide enough to be stable on the balance was build to hold the bottle with a chain.

- A balance with a range of 0-6100g and 0.01g readability and repeatability was used to measure the transferred EO sample size.

- The automatic pressure tracking adiabatic calorimeter (APTAC) is described in more detail in Chapter III.

- The APTAC test cell and transfer lines were evacuated of air using a Sargent - Welch two stage vacuum pump (Model 8804). Details: 25 LPM Free Air Displacement; 1725 rpm pump speed; Motor: 1/6 HP, 115V AC, 3.80 Amps and 60 Hz. A Bourdon gauge was installed in the line to measure the vacuum pressure.

- A nitrogen cylinder of 2200 psia was used to purge and dilute air or EO inside the APTAC cell. A low pressure N_2 regulator supplied with the EO cylinder prevented overpressure of the APTAC cell.

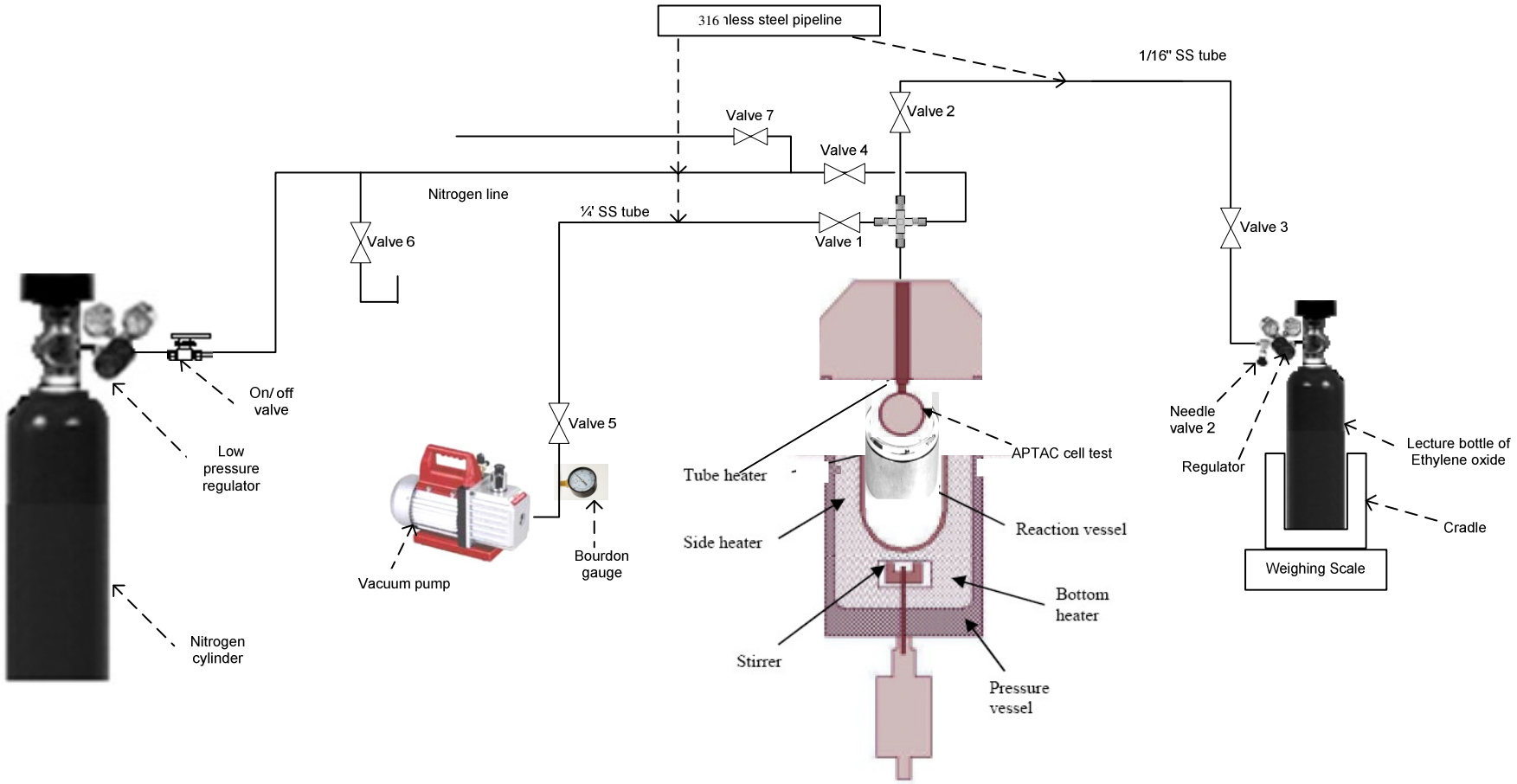

Figure 8 Schematic of transferring EO into APTAC cell

4.3 Procedures

For the present work, all APTAC experiments were performed in a closed cell environment without air above the sample. Heat-wait-search mode of operation was applied for all of the tested samples in this study. The experimental procedures consisted of the following:

First, cleaning is performed to remove contaminants in the test cell and tubing. A series of test cell and transfer line flushing with acetone were performed several times. Then, the system was dried by flushing with compressed nitrogen. Roughly 0.1, 0.5 or 1.0 g contaminants were charged into the sample cell before installing the sample cell with contaminant in the top of containment vessel. Next, a series of purging and evacuating cycles were applied to ensure the absence of oxygen from the test cell and transferring line. After evacuating, the sample vessel was kept under a vacuum pressure of about 0 psia and surrounded by a bath of dry ice acetone which was used to freeze the sample cell to −78 ◦C and enhance the EO transport process. Later, liquid ethylene oxide was collected from the lecture bottle until sufficient material was obtained in the sample cell. Following transfer of the EO, the dry ice acetone was removed. As soon as the loaded sample and reaction vessel reached a temperature of about 10^{o}C, the containment vessel was closed.

Closed –cell heat-wait-search mode of operation was applied for all of the tested samples in this study. The sample was heated to an initial search temperature depending on the expected reaction onset temperature. The temperature was allowed to stabilize for 25 minutes and the system entered the search mode to detect an exotherm thereafter (25 minutes more). Steps of 10^{o}C were conducted at a rate of 4^{o}C/min. An exothermic activity was detected when a threshold of self-heating rate of 0.05 ^{o}C/min was exceeded. Shutdown criteria were selected not to exceed a specified maximum values such as maximum temperature, maximum heat rate, and maximum pressurization rate.

At the end of each run, the sample was cooled to room temperature. A series of diluting and releasing the gas mixture inside the sample cell by compressed nitrogen gas was performed for safety.

Generally, there were no significant differences in the experiment procedures except for the preparation steps of the NH_4OH. For this contaminant, a series of purging and evacuating cycles were applied after the bottom of the sample cell was frozen using a dry ice acetone bath.

For some samples of KOH and NaOH, the experiments were repeated using either black Teflon-coated sheath thermocouple or the original unshealthed thermocouple with no measurable difference in the results. Moreover, in this work, the onset temperature of pure EO measured using the original thermocouple was around 205^{o}C which is in good agreement with that of pure EO in the literature [16, 17]. Hence, the original thermocouple was chosen for the experiments in this work.

Detected onset temperatures measured in glass and titanium test cells were the same for neat EO using the APTAC [16]. As a result, it was presumed that titanium cells, like glass cells, provided an environment without significant contamination for the EO. Because of the greater strength, titanium sample cells of 130 cm^3 nominal volume available from the APTAC manufacturer were used to perform experimental runs. The total weight of the titanium cells ranged between 30.43 and 34.56 g.

Some experiments with and without the presence of a magnetic stir bar were performed with no difference in the results. Hence, the experiments were run without the stirring bar.

4.4 Assurance of APTAC data integrity

To assure data accuracy, the following calibration tests were done any time that the sample thermocouple was replaced. Calibration was also run following every 15 tests.

4.4.1 Thermocouple calibration

Two kinds of thermocouple calibration were performed: relative and absolute.

The purpose of a relative calibration is to minimize either negative or positive drift of the system, because a small deviation between the sample and nitrogen gas temperatures can lead to substantial errors. It is shown that 1^{o}C of deviation may cause a drift rate of 0.1 ^{o}C/min at modest pressure. As a result, the thermocouple must be calibrated to within 0.1^{o}C or even less for an exotherm detection level of 0.01 ^{o}C/min [20]. The APTAC in this work was calibrated beforehand by mounting an empty and clean cell in the calorimeter. An initial pressurize of 500 psia in the vessel was chosen to run the relative calibration in this research. Besides, the other parameters were a the starting temperature of 50^{o}C, an end temperature of 460^{o}C, a cool-down temperature of 50^{o}C, and a heating rate of 4^{o}C/min. When a calibration was completed, the thermocouple offsets at 50^{o}C intervals between 50 and 400^{o}C were automatically stored. Figure 9 presents one of the thermocouple offset profiles in this work.

The absolute calibration was used to check the accuracy of the absolute temperature of thermocouple measurement. One of the easiest way to do this calibration is called the ice point check near 0^{o}C. The thermocouple zero point was adjusted periodically by placing the sample, nitrogen, and wall thermocouple in an ice/water mixture. The other way that calibration was checked is thermocouple readings. The reading values were expected to be similar for all the thermocouples when the calorimeter was in equilibrium (left without test cell overnight).

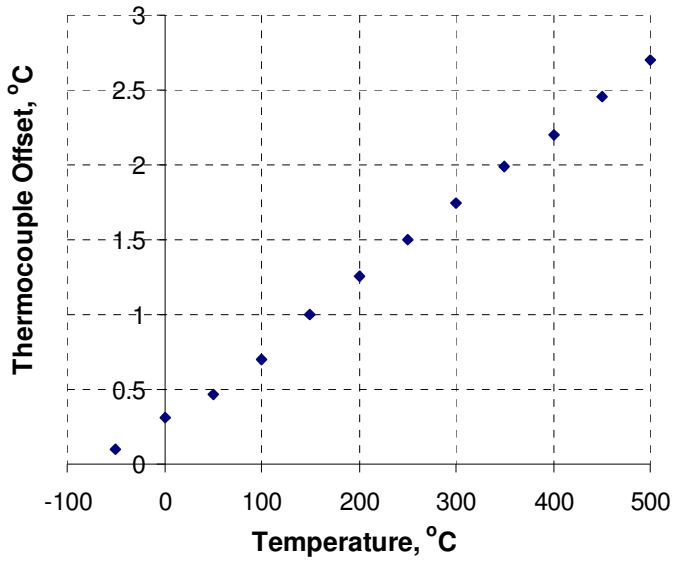

Figure 9 Thermocouple calibration

4.4.2 Pressure transducer calibration

There were two types of test performed to calibrate the sample pressure transducer: one is the water vapor pressure run and the other is di-tertiary butyl peroxide (DTBP) standard run. These tests can also be used to check the sample and nitrogen thermocouple.

A 50g sample of pure water was heated in a clean, evacuated sample cell and then allowed to cool down to ambient temperature. After the experimental run was finished, the resultant vapor pressure versus temperature was collected and compared to the literature steam table values. Figure 10 presents a water vapor pressure run and values from the steam table. As observed in this figure, the vapor pressure data values are in good agreement with that of the steam Table. This result shows the adequacy of the measured data.

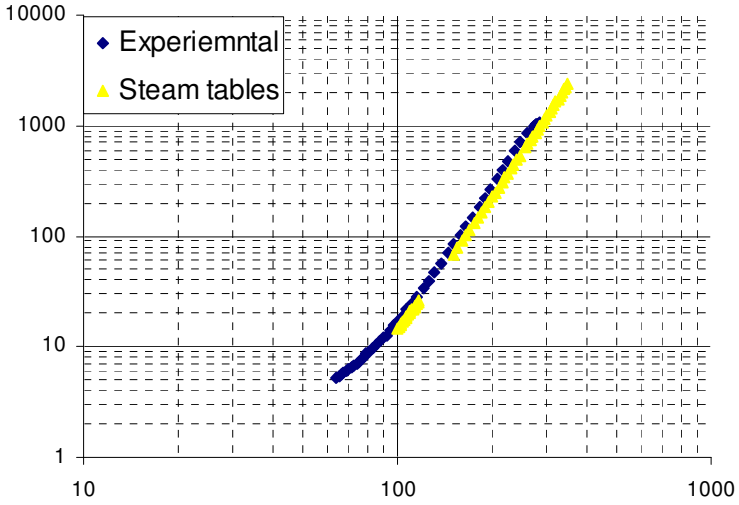

(a)

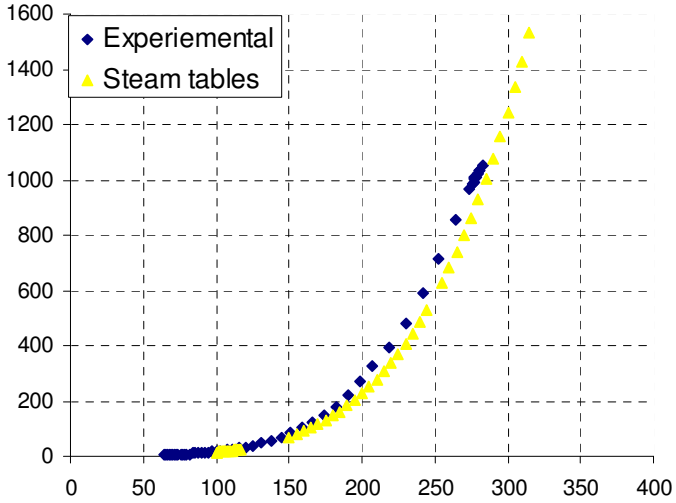

(b)

Figure 10 Water vapor pressure.
(a) logarithm scale, (b) even scale

Because there are several open literature data with the thermo characteristics of DTBP, which is a standard for calorimeter testing and comparison, 20 wt% DTBP in toluene standard was also run periodically [20, 22]. Figure 11 presents the self-heat rate profile of

the mixture 20% DTBP/Toluene compared with the APTAC standard sample heat rate. The test data are shown to be a good agreement with the open literature data.

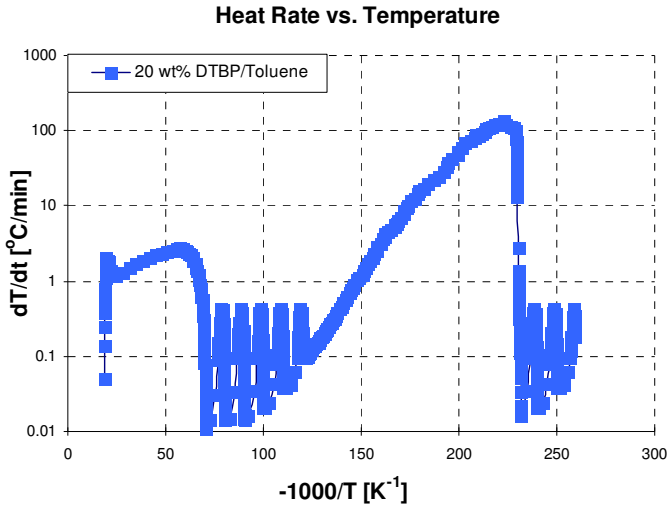

(a)

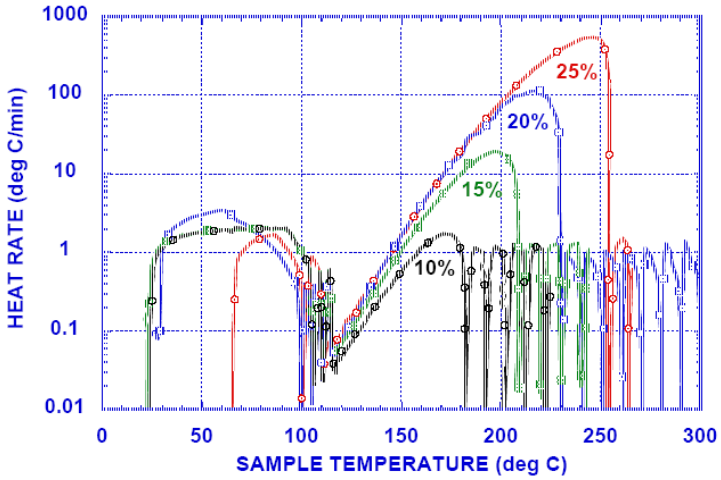

(b)

Figure 11 Self-heat rate profiles for 20 wt% DTBP in toluene. (a) Experimental; (b) APTAC manual

Figure 12 depicts the temperature versus time behavior for 20 wt% DTBP in toluene. The maximum temperature obtained at the first peak is ~ 230°C, which is in good agreement with the literature result [26].

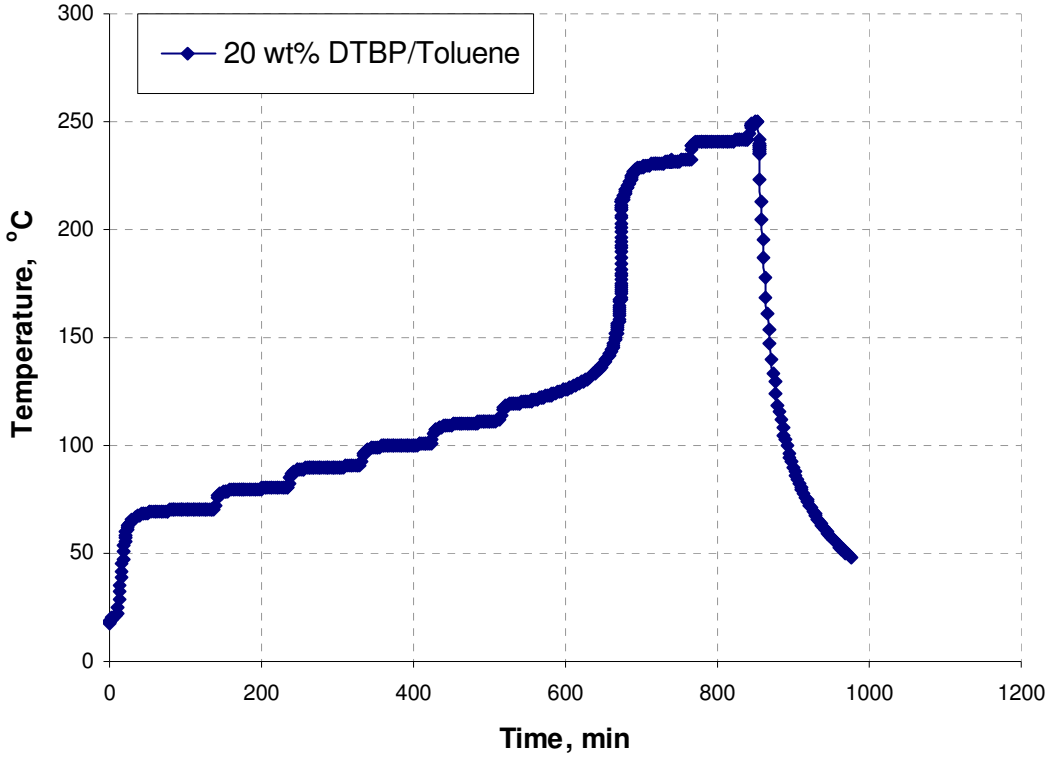

Figure 12 Temperature history of 20 wt% DTBP in toluene measured in this APTAC

4.4.3 Leak check

It is very important that the sample vessel be leak tight. A small leak from the reaction vessel during the test can cause loss of the sample and the lower sample pressure during the test.

Hence, a leak check was always conducted manually before each test. To conduct a leak test, differential pressures were created between the reaction vessel and the containment vessel. The rate of pressure rise or fall and the absolute pressure of the sample cell and the containment vessel were recorded over a period of 25-30 minutes. When a rate of pressure change of 0.01 psi/min or more was obtained, leaks were suspected and a detection solution was used to locate the leak or leaks.

4.4.4 Free contaminant environment

To prevent undesired contamination, the tubing lines between the sample cell and transducers and also the tubing leading to the on/off valves were flushed with acetone before every experiment. Then, the tubing was dried by flushing with compressed nitrogen. In addition, all items that might be involved in contamination of the samples were also cleaned carefully.

4.5 Data analysis

4.5.1 Data gathering

For each experiment, APTAC reports the following profiles: temperature versus time, pressure versus time, temperature versus pressure, heat rate versus temperature, and pressure rate versus temperature [20, 22, 25].

The onset temperature (T_{on}) and maximum temperature are indicated from the temperature versus time profiles. Onset temperatures provide information for safe storage and process temperature ranges. The maximum temperatures are used in the selection of process equipment material to ensure that the mechanical integrity of the containers or reactors will not be compromised in worst-case scenarios.

The pressures versus time profiles show the maximum pressures, which are very important in the design of safety-relief valves, since the mechanical failure of container is normally compromised by overpressure.

Maximum heat-rate and pressure-rate, which are useful in the design of safety-relief equipment, are derived from the heat-rate vs. temperature and pressure-rate vs. temperature profiles.

These curves also provide information on the time to maximum rate (T_{MR}) in the design of emergence procedures, and to prevent catastrophes. In addition to the above information, the slopes of the pressure and temperature curves mentioned above are needed for potential hazard evolution.

4.5.2 Behavioral analysis

The reactivity of KOH, NaOH, NH_4OH, and EDTA with EO were studied in this work. Comparisons of their reactivity on EO are made of the experimental results.

4.6 Phi-factors

In the APTAC, a thin-wall 2.5 in. titanium sample cell is employed to limit the amount of heat absorbed from the sample, but the sample cell still absorbs part of the thermal energy produced by the sample. A ratio of the total heat of reaction to the heat absorbed by the sample in the laboratory instrument, or expressed differently, the relative thermal capacitance of the cell plus sample to the sample alone is expressed by the phi-factor, Φ [20, 27, 28]:

$$\Phi = 1 + (m_c C_c)/ (m_s C_s) \qquad \textit{Eq. 1}$$

Where m_c (g) is the sample vessel mass

C_c ($Jg^{-1}K^{-1}$) is the sample vessel specific heat

m_s (g) is the sample mass

C_s ($Jg^{-1}K^{-1}$) is the sample specific heat

The phi-factor has the effect of dampening the magnitude of a real system. The relative wall thermal capacitance might be very small in the case of the large-scale equipment.

Hence, the higher phi-factor of the laboratory instrument results in a lower observed temperature rise, a lower pressure rise, but a higher onset temperature [29].

Therefore, phi-factor is an important issue for scaling laboratory results to industrial processes, where Φ factors typically are low. The "corrected" values can be derived from the measured ones using the following equation [20, 25, 27, 28]:

$$(T_{max} - T_o)|_{adj} = \Phi * (T_{max} - T_o)|_{meas}$$

The onset temperature and the self-heating rate of the reaction measured at any Φ factor is adjusted to a new value at any Φ using the following equations suggested [27, 28]

$$\frac{1}{T_{o,2}} = \frac{1}{T_{o,1}} + \frac{R}{E_A}\ln(\frac{\Phi_1}{\Phi_2}) \qquad \textit{Eq. 2}$$

$$\left.\frac{dT}{dt}\right|_{\Phi_2} = \left(\frac{\Phi_1}{\Phi_2}\right)\exp\left[\frac{E_A}{R}\left(\frac{1}{T_{\Phi_1}} - \frac{1}{T_{\Phi_2}}\right)\right]\left.\frac{dT}{dt}\right|_{\Phi_1} \qquad \textit{Eq. 3}$$

The maximum temperature are also corrected as follows

$$T_{max} = T_{o,adj} + \Phi\,\Delta T_{meas}$$

Lastly, Wilcock and Rogers suggests the equation to correct the time to maximum rate under adiabatic condition [26]

$$T_{MR_{adj}} = \frac{T_{MR_{meas}}}{\Phi}$$

Hence, to adjust the current study's results properly for equipment with a lower phi-factor, a dynamic simulation that takes into account the observed reaction kinetics coupled with material and equipment properties would be required.

In this work, phi factors can not be measured directly by the APTAC and was calculated using the equation 1. The average heat capacity of EO used in the phi-factor calculation of 2.0 $J/g^{-1}K^{-1}$ was derived from the literature [16]. The average heat capacity of titanium

was estimated to be 0.569 $J/g^{-1}K^{-1}$ [31]. In these research experiments, the phi factor in this research ranges between 1.58 and 1.66.

4.7 Uncertainties

The thermocouple was used to measure sample temperatures with an overall absolute uncertainty of ~ ± 1 ^{o}C [22], and was periodically checked at 0^{o}C using an ice bath. Sample pressures were frequently checked for agreement with the water vapor pressures and the ambient pressures. Sample weights were measured with accuracy to within ± 0.01 gr. Sample cell volumes were within ± 5 cm^3 of 130 cm^3.

CHAPTER V

RESULTS AND DISCUSSION

In this chapter, the experimental data are presented. The results and discussion are categorized into five sections: the reactivity of pure EO, EO and the contaminants including potassium hydroxide, sodium hydroxide, ammonia hydroxide, and EDTA and a comparison section.

For each contaminant, three scenarios with different contaminant amount (0.1, 0.5, and 1 gram) are investigated. Several graphs were generated by the APTAC and are reproduced here. At the end of each section is a summary table to report important information derived from the graphs, including onset temperatures, maximum temperature and pressure, maximum temperature and pressure rates and time to maximum rate along with respective uncertainties corresponding to one standard deviation of the experimental replicas. The value of onset temperature self-heat rate reported here is about 0.1^{o}C/min, which approaches the detection limit of the APTAC. The time to maximum heat rate, t_{MR}, estimates the time available to prevent a possible catastrophe from the moment that a heat generation rate of 0.1^{o}C/min is detected.

5.1 Pure ethylene oxide

In order to successfully understand the reactivity of EO with the contaminant or the contaminant effects on pure EO, it is necessary to know the neat ethylene oxide behavior in the absence of contaminants.

The reactivity of pure EO investigated using the APTAC exhibited considerable exothermic activity. Temperature profiles for pure EO are shown in Figure 13. Despite the programmed heater shutdown for 500^{o}C for all of these tests, temperatures in excess

of 580°C were achieved in all cases. Pure EO reached an onset temperature of 205°C, which is in good agreement to the results of the previous research [16, 18].

The corresponding pressure-time relationships appear in Figure 14. By the end of the tests, pressure reached approximately 1700 psia.

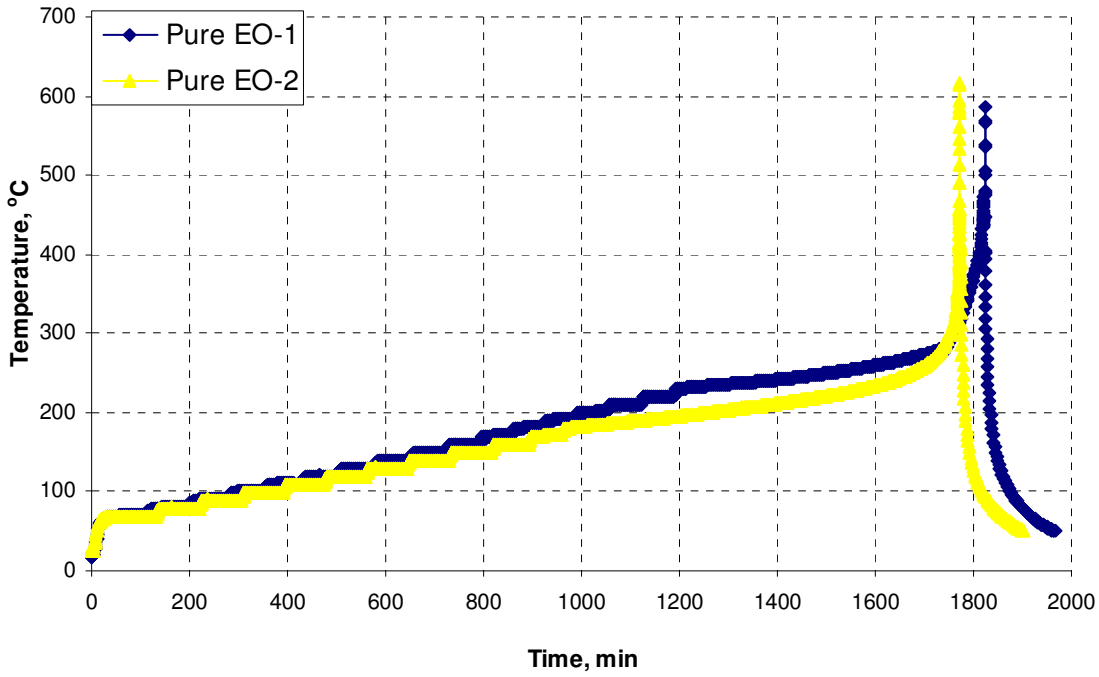

Figure 13 Temperature history of pure EO in the APTAC

The self-heat rate behavior appears in Figure 15. Heat rates approaching approximately 1700 °C/min were observed.

The experimental results are summarized in the Table 5. The uncertainties are also reported corresponding to one standard deviation of the experimental replicas.

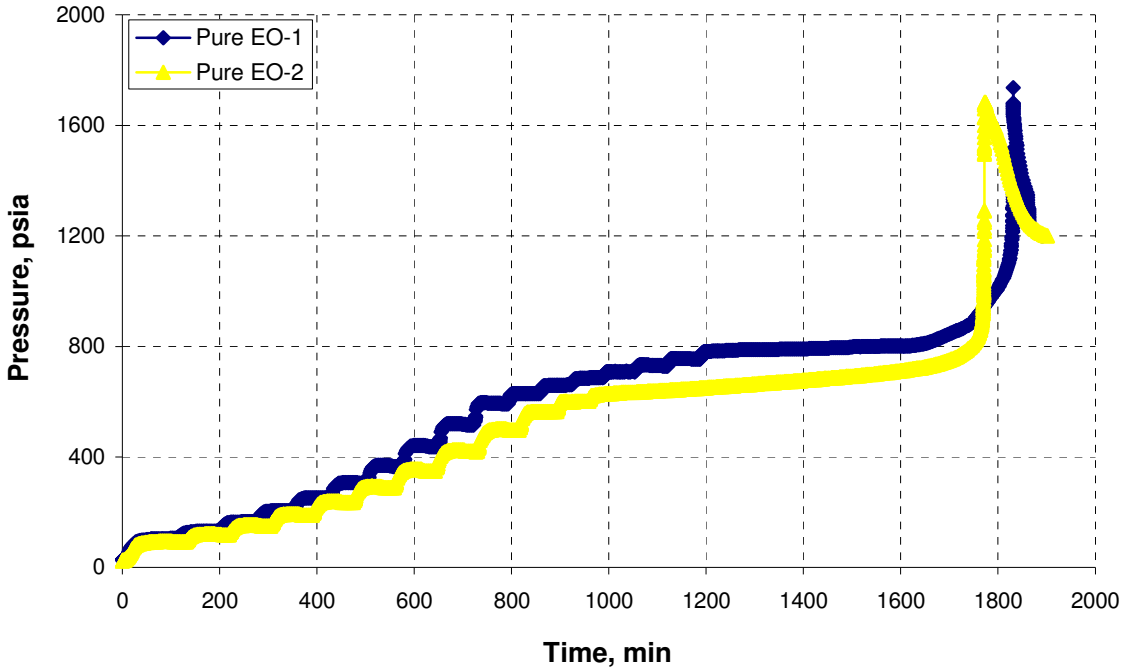

Figure 14 Pressure history of pure EO in the APTAC

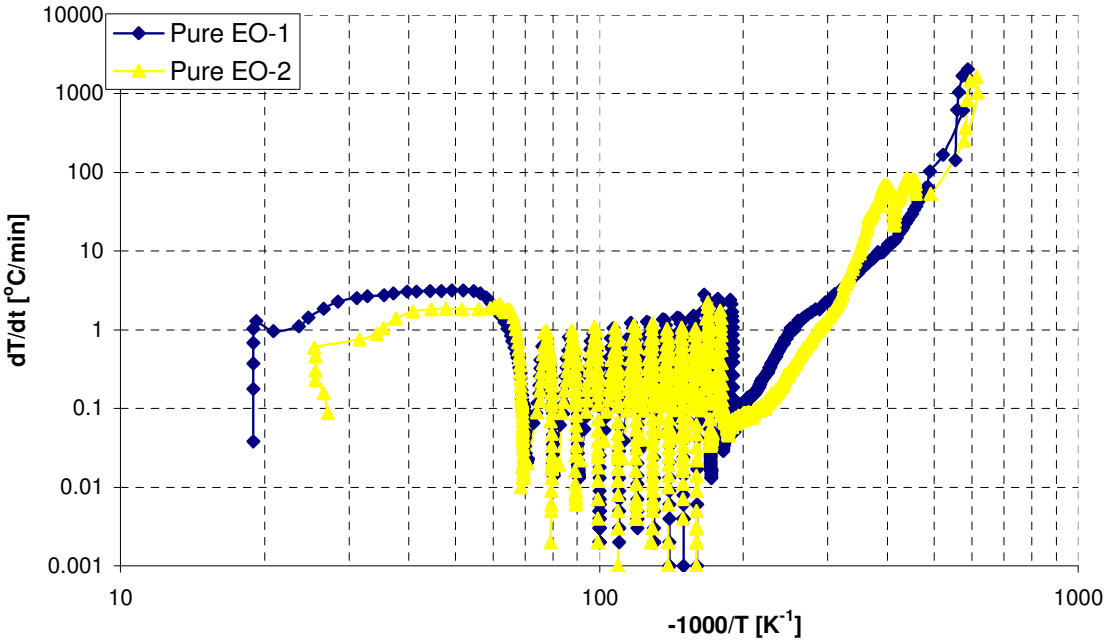

Figure 15 Self-heat rate profiles of pure EO in the APTAC

Table 5 Experimental results of APTAC analysis on pure EO samples

	Φ	T_{on} ^oC	T_{max} ^oC	P_{max} *psia*	dT/dt_{max} $^oC/min$	dP/dt_{max} *psi/min*	T_{MR} *min*
EO	1.64	205 ± 16	600 ± 13	1709 ± 27	1694 ± 49	3859 ± 75	296 ± 27

5.2 Ethylene oxide in contact with potassium hydroxide (KOH)

The combination of EO with potassium hydroxide (KOH) was investigated since this contamination is possible in a manufacturing process. Three experimental scenarios with different contaminant amounts (0.1g, 0.5g and 1.0g KOH) and 14g EO were conducted. The run data are presented in Figure 16 to Figure 21 and Table 6. The reproducibility of the experiments can be clearly observed in these graphics.

Figure 16 depicts the temperature - time curves. For an amount of only 0.1g KOH, the data reveal an exotherm beginning at approximately 50^{o}C, much lower than that of pure EO at 205^{o}C. The heat onset temperature decreases with an increase of KOH concentration. For the 1.0g KOH contamination scenario, an exotherm appears at around 30^{o}C, near the minimum starting temperature of the APTAC. This figure also shows that the mixture inside the cell eventually reaches a maximum temperature of around 160^{o}C, 220^{o}C, or 230^{o}C in the case of contaminated mass 1.0g, 0.5g, and 0.1g KOH, respectively. The trend of increasing the maximum temperature by decreasing the concentration of KOH is clearly reflected in the range of 0.7 – 7.07 % contaminant weight.

The plot of pressure – time curves (see Figure 17) also indicates that an exotherm occurs shortly after contact of EO with a contaminant, starting at the beginning of experiment and ending with maximum pressures of up to 550 psia in the scenario of 1.0g KOH contaminant. The maximum pressures decrease as the concentration of the contaminant KOH is increased.

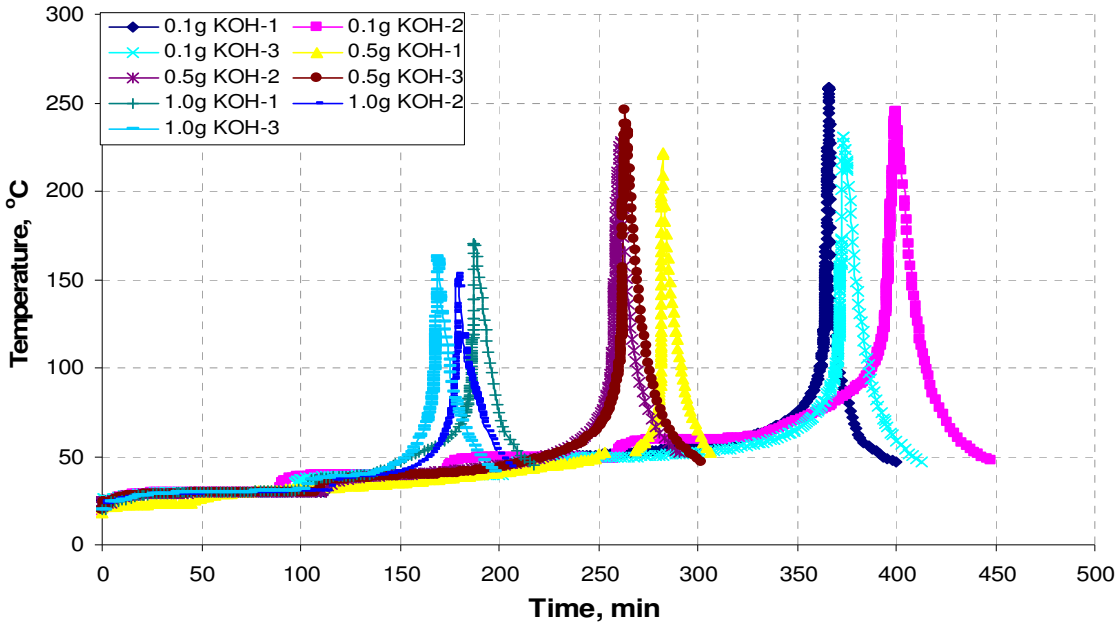

Figure 16 Temperature history of ethylene oxide and KOH

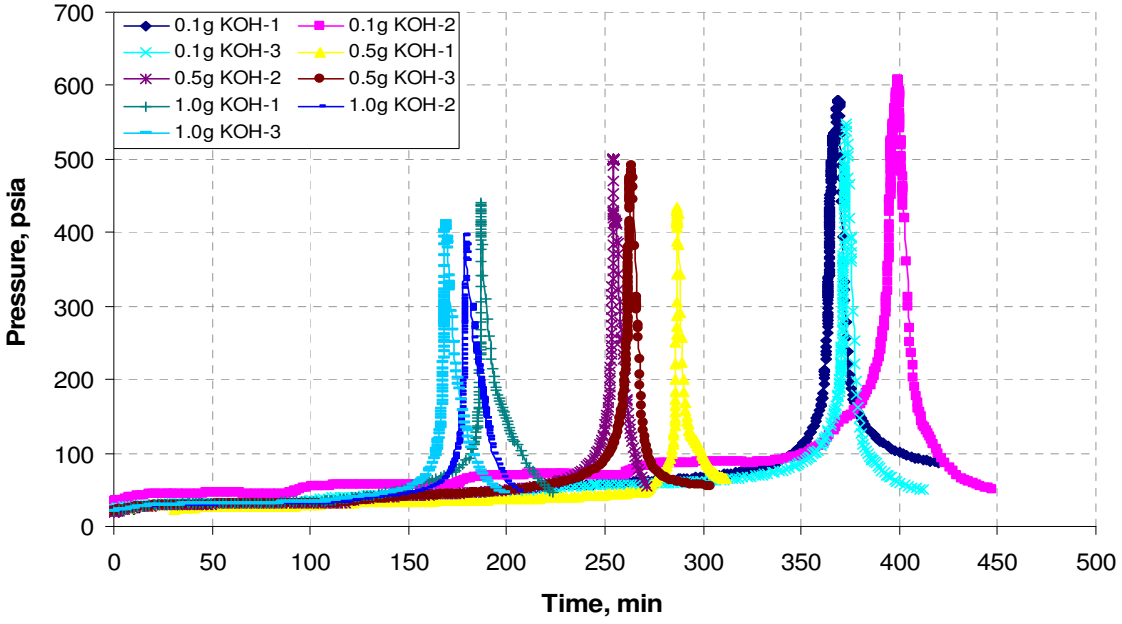

Figure 17 Pressure history of EO/KOH

The measured heat rates with respect to temperatures are displayed in Figure 18. In this figure, it can be seen that the more the contaminant KOH added, the sooner the exotherm of the sample starts, i.e. the EO stability is lowered by the increase of KOH contamination. For the scenario of 1.0g KOH contamination, the self-heat rate of over 0.1^{o}C/min is observed at room temperature. Thereafter, acceleration to around 600^{o}C/min takes place. The reaction initiates so rapidly from room temperature while the instrument is attempting to stabilize an adiabatic condition that the heaters do not increase rapidly enough for the nitrogen containment vessel temperature to match the sample temperature. For the 0.1g KOH, it is not clear if the leveling off or decrease in the self-heat rate curves is actually a reaction phenomenon or just an antifact of the tests. The maximum rates of heat generation are around 291, 620 and 577^{o}C/min for the scenarios of 0.1g, 0.5g and 1.0g KOH contaminant, respectively. It appears that there are no significant differences in the maximum heat generation rates between the two different concentration of the contaminant KOH corresponding to 0.5 and 1.0g KOH.

Parallel trends are exhibited in the pressurization rate versus temperature plots in Figure 19. There was no significant difference observed among the maximum pressurization rate in the investigated range of contaminant concentration. The pressure-temperature curves (see Figure 20) indicate the characteristic of the vapor components in the cell. The curves are divided into three main parts:

(1) Heating and exotherm: the curve slopes are straight lines, following the projected curve of ethylene oxide vapor pressure when the mixture is heated by the surroundings and the reaction energy.

(2) Then, near the end of exotherm, the pressures from these tests fall away from the projected pressure and the curve slopes are lower. In this stage, the exothermic reactions strongly released heat and increase the mixture temperature, while the pressure did not increase which is attributed to the ethylene oxide consumption.

(3) During cool-down, both pressure and temperature decreased due to the complete consumption of EO and the heaters were turned off. The curves are not straight lines because some products condensed at the beginning of this period. The fact that the cooling curve slopes are lower than the heating curve slopes indicates that EO was converted into less volatile components. The reaction products are polymers because of polymerization reactions in the presence of KOH [31].

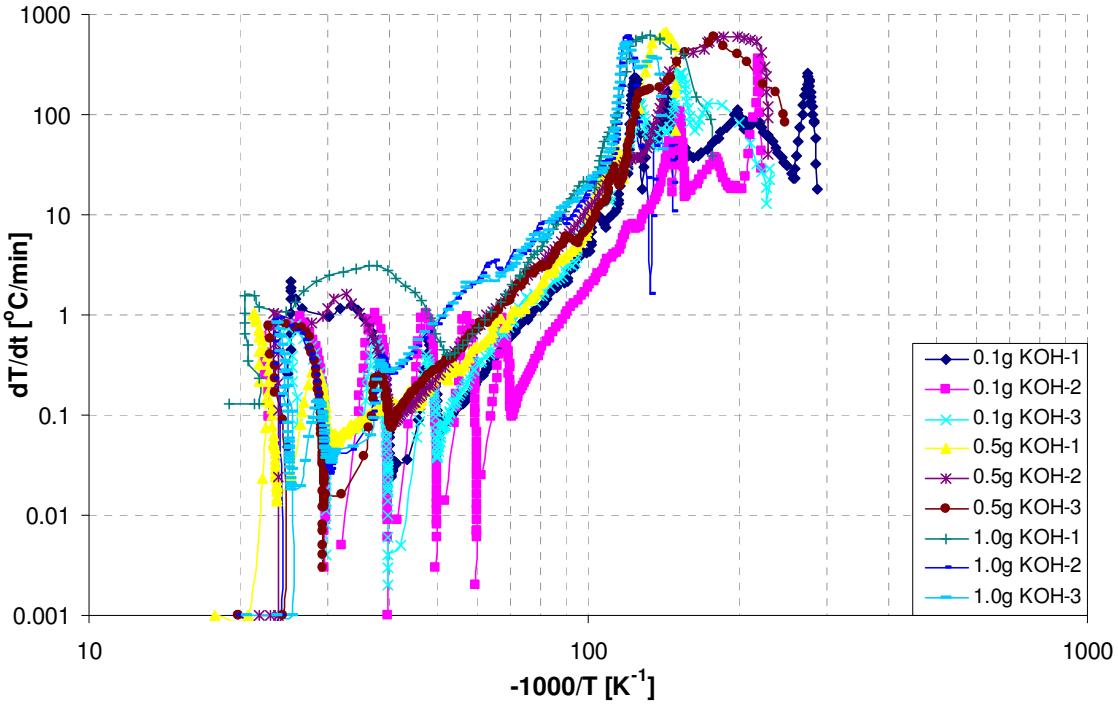

Figure 18 Self-heat rate-temperature profiles of EO/KOH

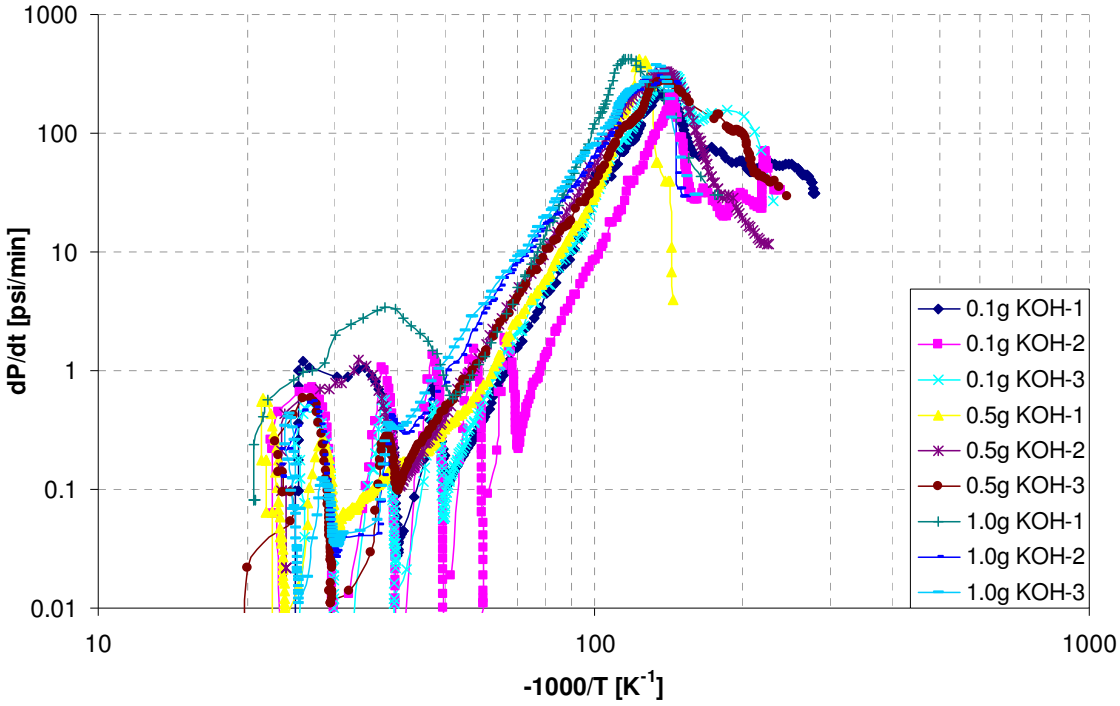

Figure 19 Pressurization rate profiles of EO/KOH

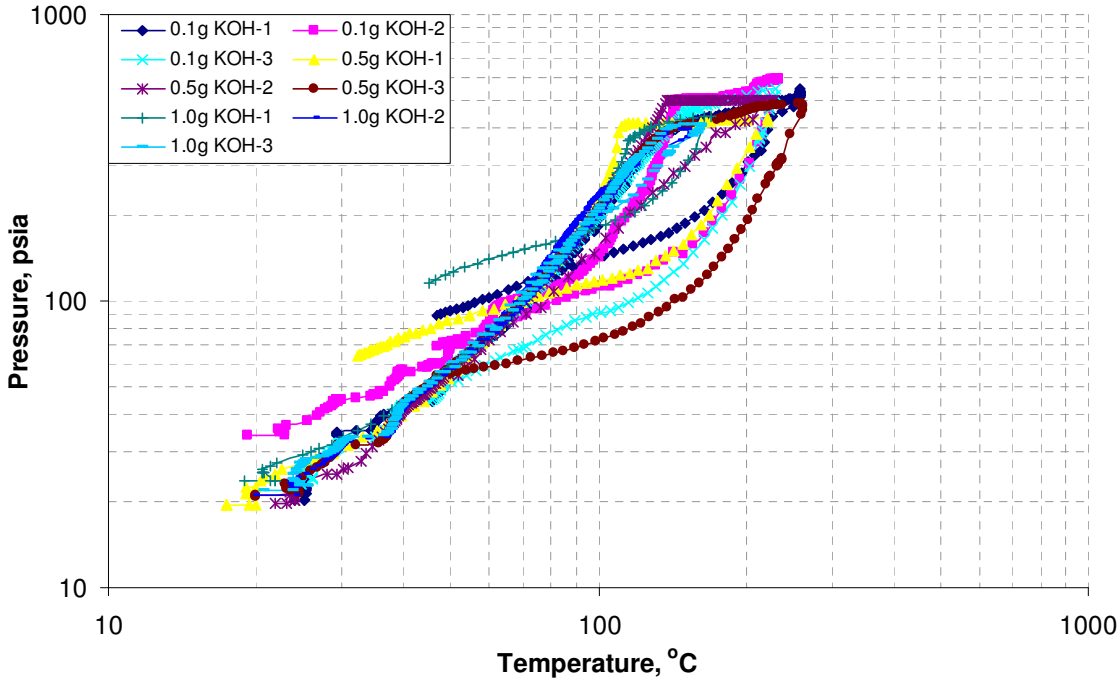

Figure 20 Pressure-temperature profiles of EO/KOH samples

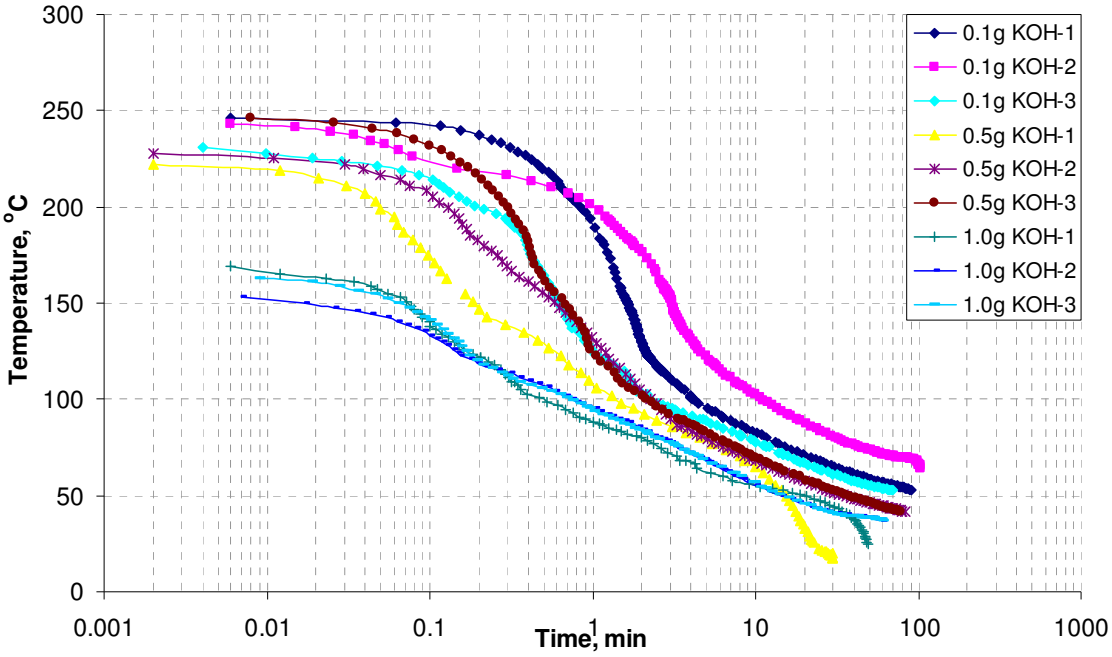

Figure 21 Time-to-maximum rate profiles of EO/KOH samples

The rapidity of the exotherm of ethylene oxide in the presence of KOH is illustrated in the time-to-maximum rate plot of Figure 21. In the case of 1.0g KOH, at near ambient temperature, it takes around 60 min for the rate to reach its maximum, but by 60°C, the time to maximum rate is only about 10 minute. For the smaller amount of the contaminant KOH, more time is needed for the heat rate to reach its maximum.

A summary of important parameters in the experimental results with contaminant KOH is presented in Table 6. The presented uncertainties are within one standard deviation based on three replicas. When the contaminant concentration increases, the onset temperatures, maximum temperature rates, maximum pressure rates tend to more dangerous values, i.e., EO mixture is more hazardous, although the maximum temperature and maximum pressure decrease.

Table 6 Experimental results of APTAC analysis on EO/KOH mixtures

Contaminant	Φ	T_{on} ^{o}C	T_{max} ^{o}C	P_{max} *psia*	dT/dt_{max} $^{o}C/min$	dP/dt_{max} *psi/min*	T_{MR} *min*
0.1g KOH	1.65	57 ± 5	240 ± 7	575 ± 20	291 ± 48	238 ± 44	88 ± 14
0.5g KOH	1.62	40 ± 2	231 ± 10	475 ± 28	620 ± 30	342 ± 58	78 ± 3
1.0g KOH	1.61	34 ± 3	162 ± 7	418 ± 18	577 ± 48	385 ± 28	58 ± 3

5.3 Ethylene oxide in contact with sodium hydroxide (NaOH)

The reactivity of EO in contact with the contaminant sodium hydroxide in three scenarios (0.1g, 0.5g and 1.0g NaOH) was also probed. The experimental data are presented in Figure 22 to Figure 27 and summarized in Table 7.

Figure 22 depicts the temperature curves with respect to time. For the NaOH contamination, the exothermic phenomena occurred at over 100^{o}C, much higher than that of the KOH contamination. As the contaminant concentration increases, the averaged onset temperature slightly decreases, although it is not clearly seen as in cases with contaminant KOH. The maximum temperatures with NaOH were around 200^{o}C – 230^{o}C. Similar trends are also seen in pressure-time behavior (see Figure 24). The pressure data parallel the trends displayed in the temperature versus time plots.

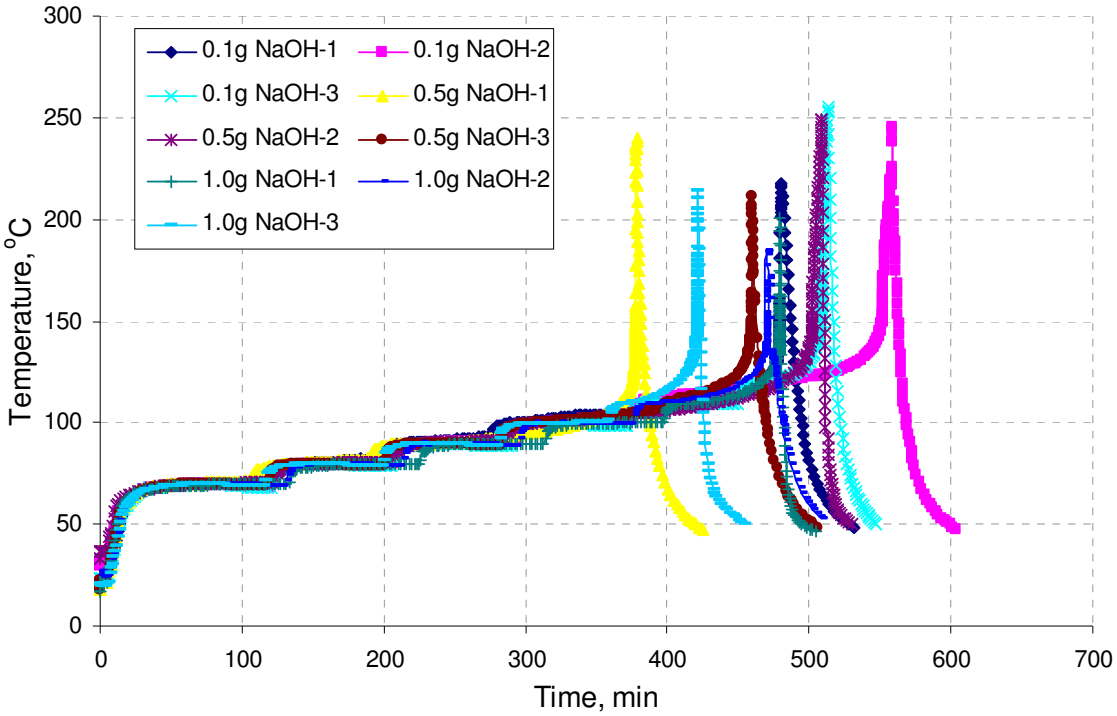

Figure 22 Temperature history of ethylene oxide and NaOH

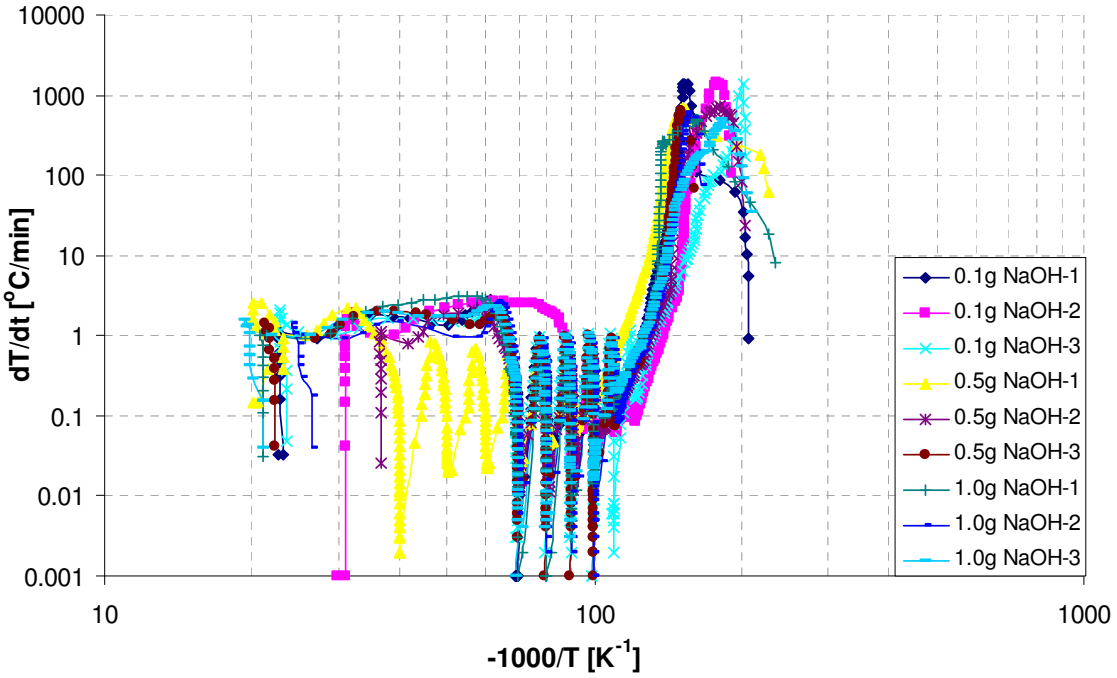

Figure 23 Self-heat rate profiles of EO/NaOH

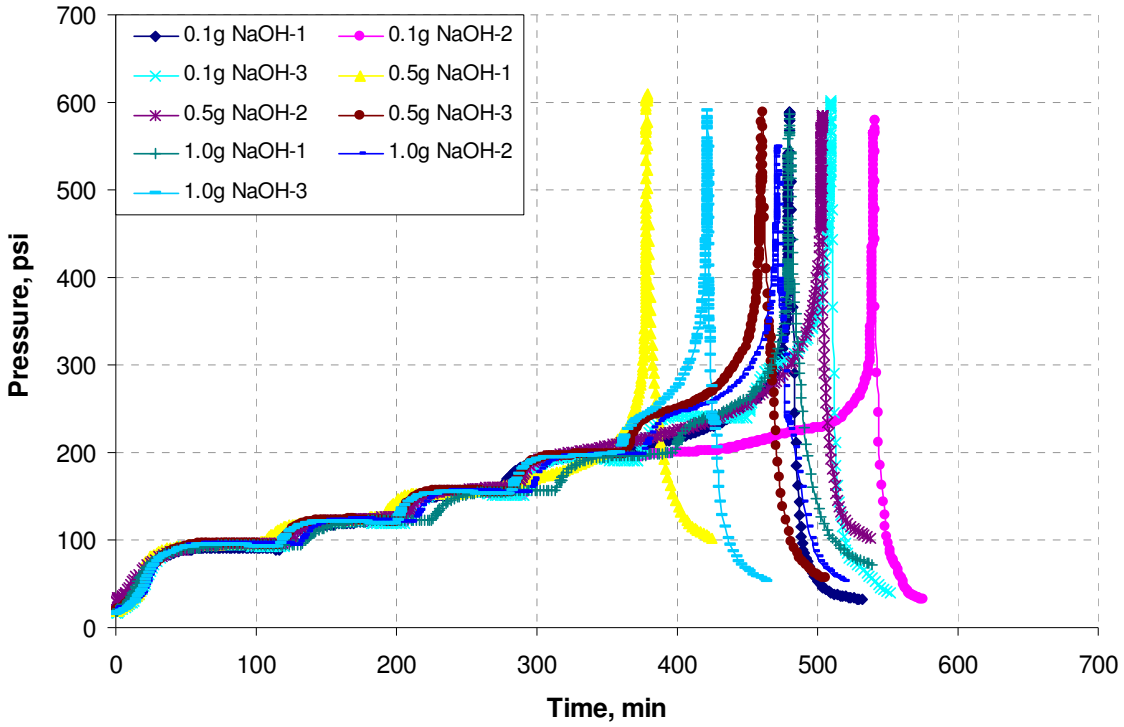

Figure 24 Pressure history of EO/ NaOH samples

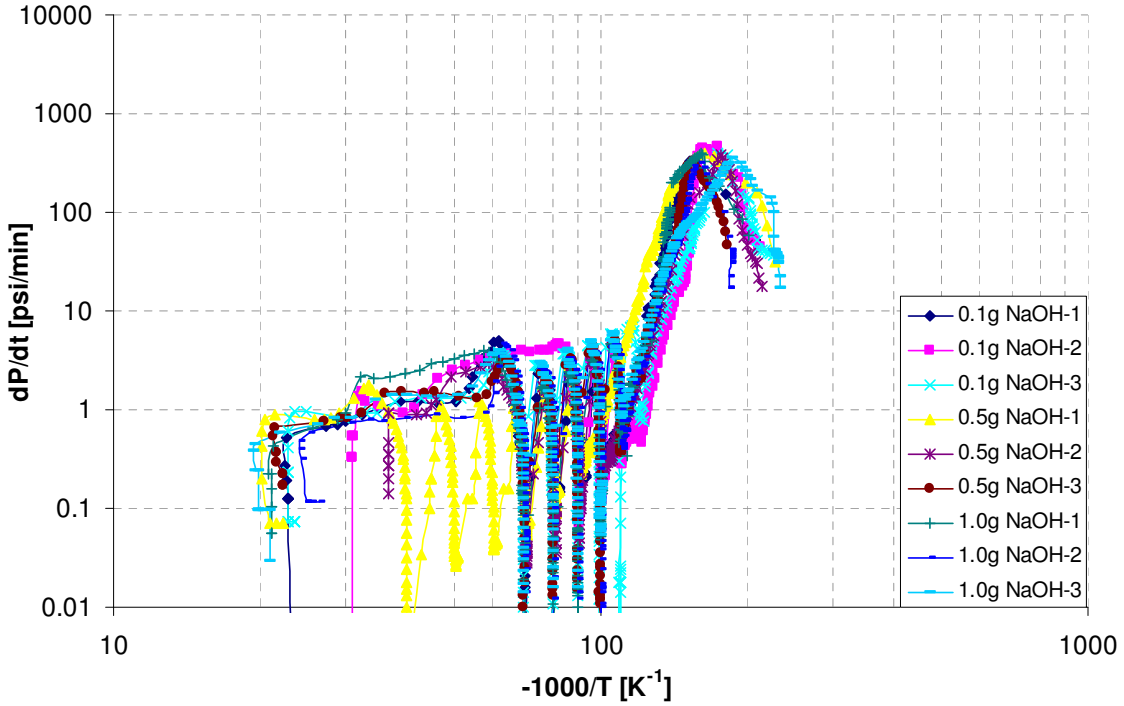

Figure 25 Pressurization rate profiles of EO/NaOH samples

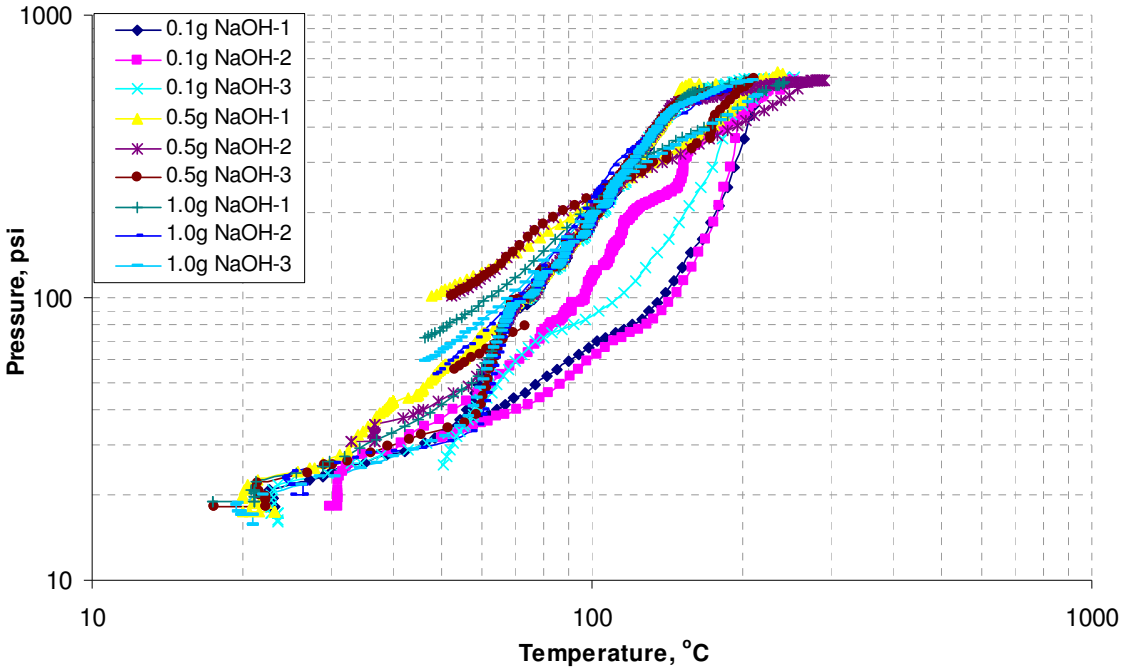

Figure 26 Pressure-temperature profiles of EO/ NaOH mixtures

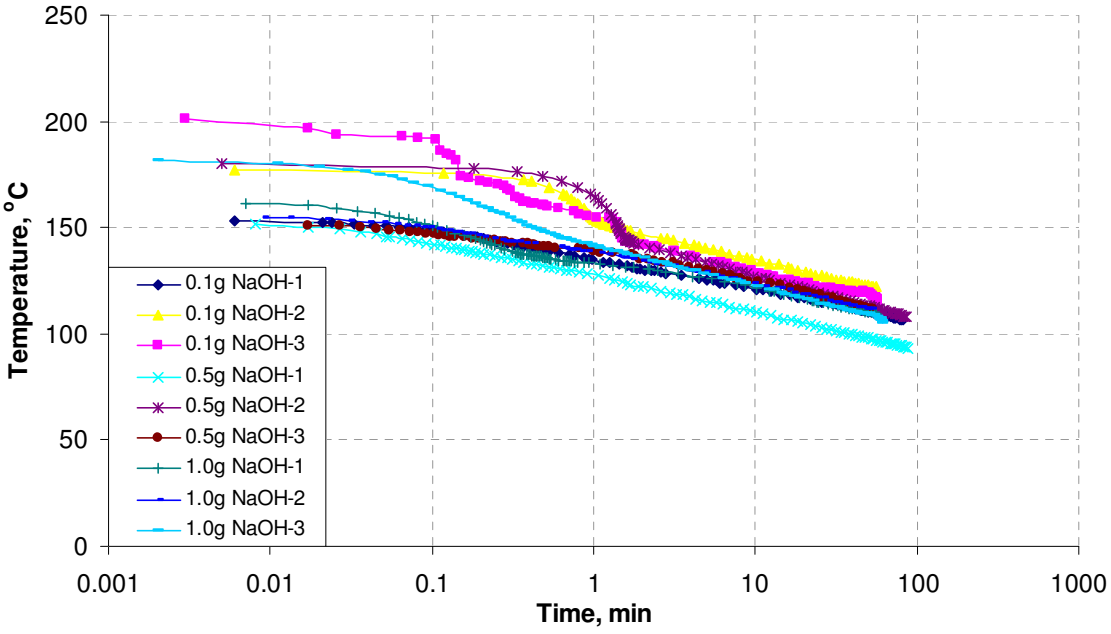

Figure 27 Time-to-maximum profiles of EO/ NaOH samples

Figure 23 illustrates the self-heat rate profiles for the samples EO/ NaOH. The self-heat rates of over 0.1°C/min were observed at over 100°C, much higher than that of the contaminant KOH. Acceleration to the average values of 1401, 679, and 526°C/min were obtained for the scenarios of 0.1, 0.5, and 1.0g, respectively. EO exotherms with lower NaOH concentrations exhibited slightly greater self-heat rates.

The pressures versus temperature plots in Figure 26 have the same behaviors as described in the cases of KOH contamination that generated the condensable products. These observations for the case of KOH and NaOH are in good agreement with the fact that strong alkali is the catalysts for the polymerization reaction of EO, releasing high energy of approximately 900 Btu/lb of reactant at certain temperatures [19].

For this contaminant, the trends of the main parameters such as the onset temperature, the maximum temperature, the maximum heat rate, the maximum pressurization rate are difficult to realize in the above plots. They are more clearly shown in the following summary table. Only two parameters including onset temperature and time to maximum heat rate tend to more hazardous values. The onset temperature decreased by 15°C as the NaOH concentration increased 10 times from 0.1g to 1.0g. The time to maximum heat rate reduced from 65 to 56 minutes, respectively. The other parameters T_{max}, P_{max}, and dP/dt_{max} slightly decreased with respect to an increase of contaminant concentration, while dT/dt_{max} reduced within a wide range.

Table 7 Experimental results of APTAC analysis on EO/NaOH mixtures

Contaminant	*Φ*	T_{on} °C	T_{max} °C	P_{max} psia	dT/dt_{max} °C/min	dP/dt_{max} psi/min	T_{MR} min
0.1g NaOH	1.64	120 ± 5	239 ± 16	599 ± 2	1401 ± 15	391 ± 48	65 ± 12
0.5g NaOH	1.62	108 ± 3	233 ± 16	594 ± 11	679 ± 40	365 ± 29	62 ± 2
1.0g NaOH	1.60	105 ± 2	200 ± 12	576 ± 19	526 ± 46	359 ± 38	56 ± 4

5.4 Ethylene oxide in contact with ammonia hydroxide (NH_4OH)

Ammonia hydroxide solution is the third basic contaminant investigated in this research. In this present work, different amounts of ammonia in the form of 30% aqueous solutions were added to 14.0g of pure EO to measure their reactivity. In the presence of water, EO reacts with water to produce higher molecular weight glycols. The lowest onset temperature for neat EO in the presence of water is approximately 60^{o}C at 25-38% weight percent water [18]. However, in this work, the onset temperature with 5% weight percent water (1.0g NH_4OH 30%) were detected at approximately 21^{o}C, much lower than 60^{o}C, which is the lowest measured onset temperature of EO contaminated by water. From the above information, it is supposed that NH_4OH is component that reduced the onset temperature, and increased the maximum temperature, maximum pressure, maximum heat-rate, and maximum pressurization rate of pure EO in this research. As a result, contamination of NH_4OH 30% was a good choice to study the reactivity of pure EO and can compare with the other contaminants.

Three scenarios with various masses of NH_4OH (0.1g, 0.5g and 1.0g) were carried out. Unlike the contaminants in the previous sections, which are anhydrous hydroxides, this basic solution contains a highly volatile compound, NH_3, dissolved in water. Both ammonia and water are present in the vapor mixture and contribute to a higher vapor pressure in the titanium cell.

From Figure 28, the EO mixtures with a higher NH_4OH concentration produced a lower onset temperature and lower maximum temperature. In the scenario with 0.1 g NH_4OH, the stair-step behavior can be seen until the mixture temperature reached about 160^{o}C. This relatively high onset temperature indicates that EO in contact with a 0.7% weight of contaminant NH_4OH is still stabilized near ambient temperature. However, the onset temperature reduced quickly to 21oC when the contaminant amount was increased 10 times to 1.0g. Although the maximum temperature in the latter scenario is much lower, this scenario is more dangerous because EO reacts at ambient conditions.

As mentioned earlier, the contaminant consisting of ammonia and water has a high contribution to the mixture pressure. Consequently, the pressure rates which were over 3000 psi/min overwhelmed the responding speed of the APTAC control system in the scenarios with 0.1g and 0.5g NH_4OH. As a result, the cells were ruptured or forced out of the head of the containment vessel. The measured pressure at the peaks should be the pressure in the containment vessel. Hence, the real final pressures creating by the contamination of 0.1g and 0.5g NH_4OH may be higher in the 130ml cell than the final pressure reported in this work. In the scenario with 1.0g NH_4OH, the reaction heat and sample pressure was not enough to rupture the cells.

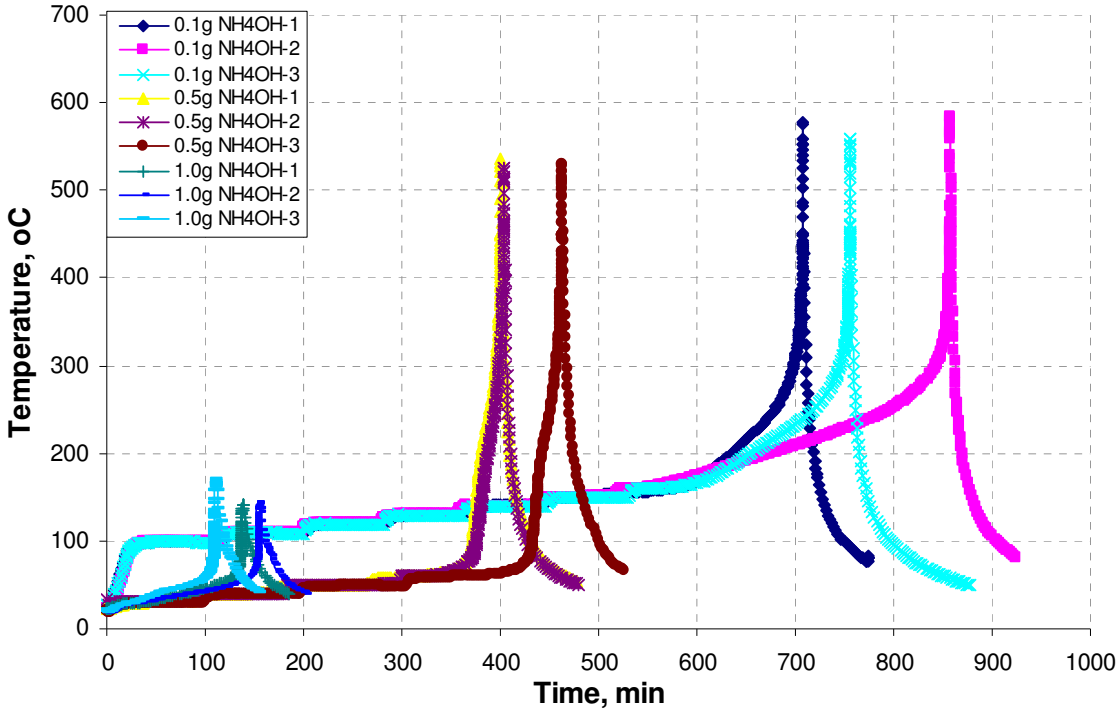

Figure 28 Temperature history of EO/ NH_4OH samples

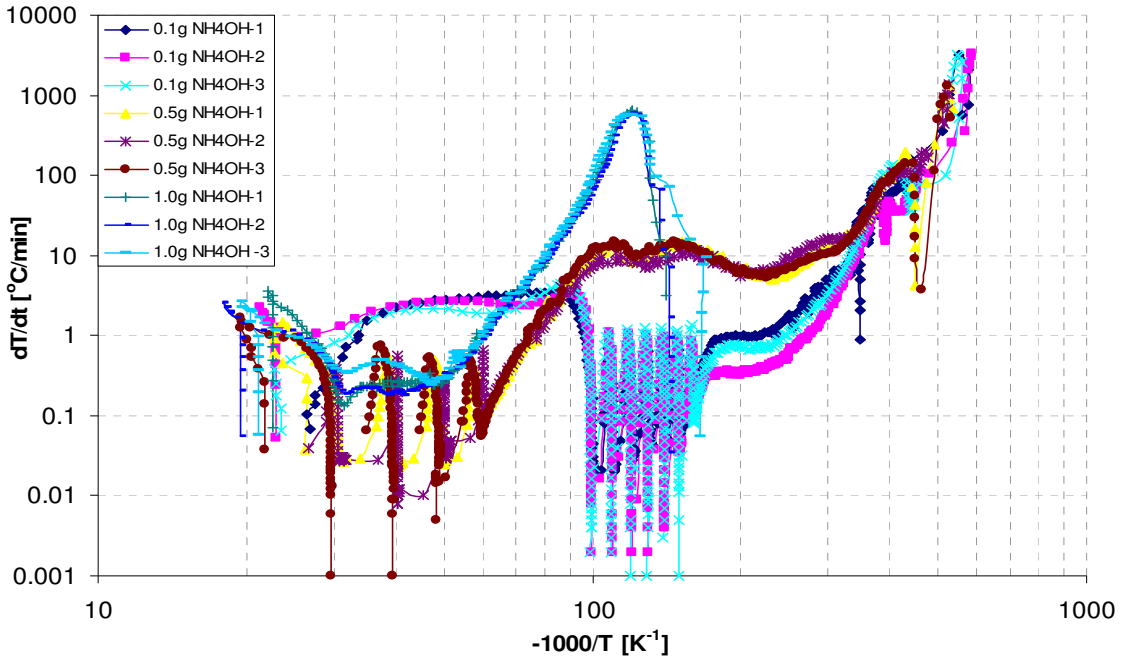

Figure 29 Self-heat rate profiles of EO/ NH_4OH samples

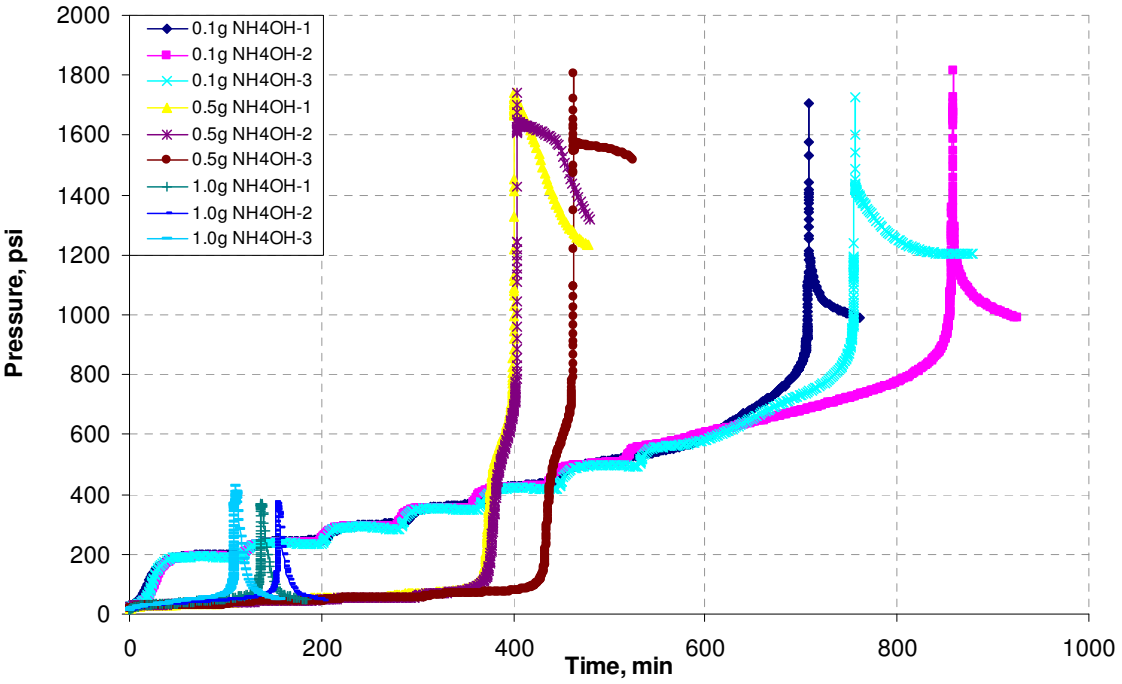

Figure 30 Pressure history of EO/ NH_4OH samples

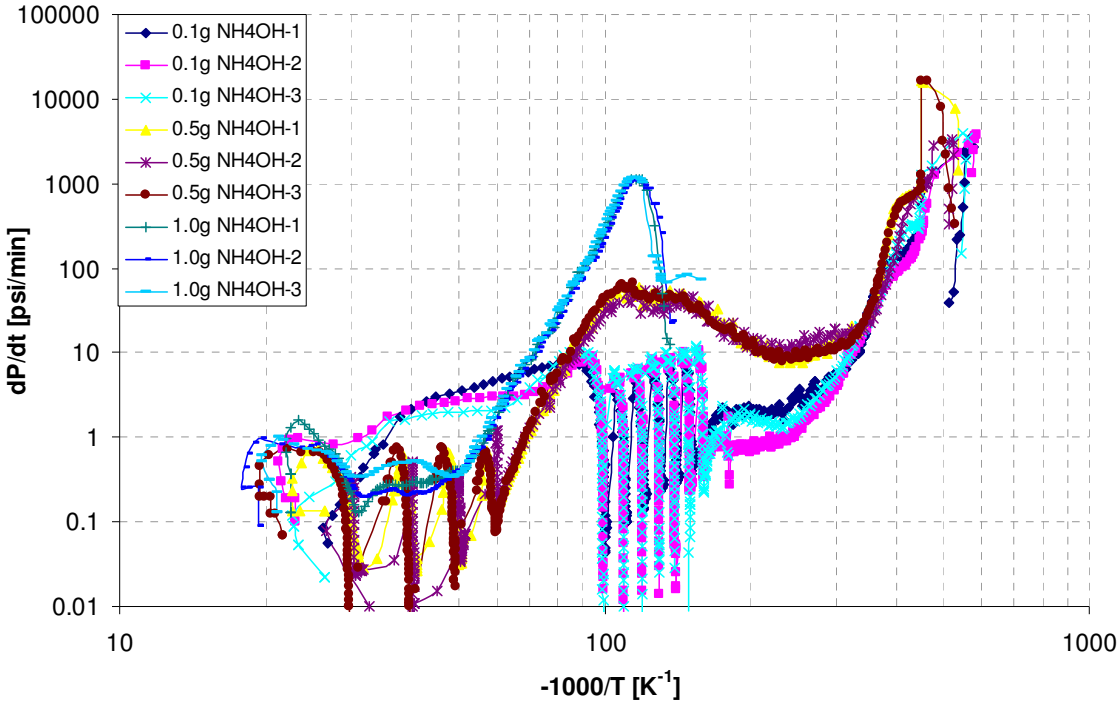

Figure 31 Pressurization rate profiles of EO/ NH_4OH samples

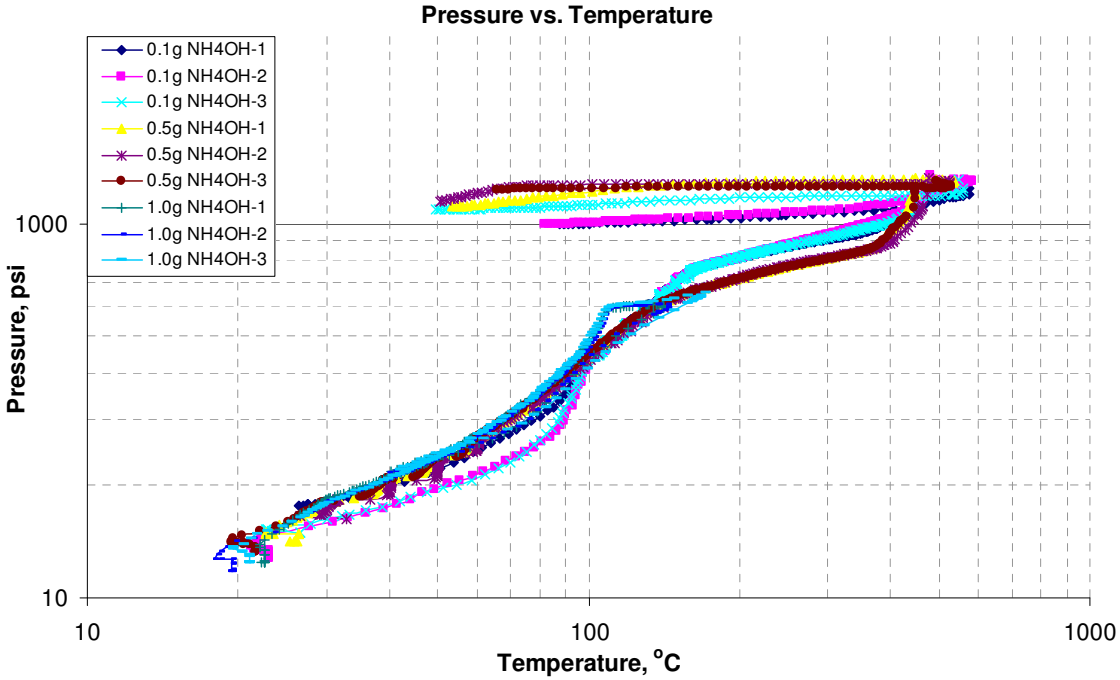

Figure 32 Pressure-temperature profiles of EO/ NH_4OH samples

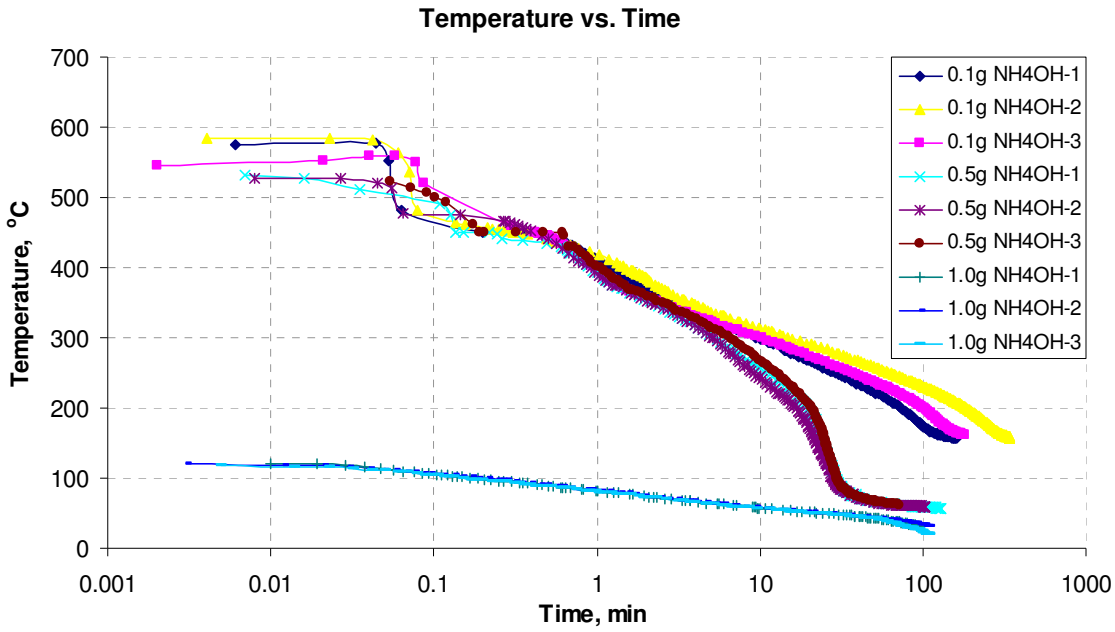

Figure 33 Time-to-maximum profiles of EO/ NH_4OH samples

Figure 29 illustrates the self-heat rate profiles of EO/ NH_4OH mixtures. The NH_4OH had a detectable exotherm at approximately 60°C, increasing to nearly 10°C/min around 100°C. The self-heat rate remained nearly constant until about 280°C and began to accelerate thereafter, giving a self-heat rate up to 150 °C/min at 430°C in the small peak, and then dropping off, until the other stronger exotherm started at 450°C, reaching a bigger peak of roughly 1300 °C/min.

The peak pressure of over 1700psi was generated in the case of 0.1 and 0.5g NH_4OH (Figure 30). And there is a phenomenon that their pressures were still high despite the cooling period had ended. This is due to the mixture ignition, following the rupture of the titanium cell and probably creating the less volatile products.

The pressurization rate-temperature profiles (Figure 31) reveal sharp increases in pressurization rate at about 450°C of the tests of 0.5g NH_4OH-1 and 0.5g NH_4OH-3. Furthermore, the titanium cells ruptured with subsequent bursting of the containment

vessel rupture disk in several tests were observed near the end of these tests. Those observed indicators suggested that ignition might have occurred.

There is an interesting observation for this contaminant. There exists a small peak right before the main peaks. They can be seen clearly in Figure 28 and Figure 30 for the scenario with 0.5g NH_4OH. Besides, several peaks are also apparent in the heat rate and pressurization rate (see Figure 29 and Figure 31). These peaks can be explained as follows:

(1) First, the initial peaks reflect the reaction between ammonia in the form of an aqueous solution and ethylene oxide to produce ethanolamine with the water acting as catalyst [32]. The combination of EO and ammonia initially produces MEA. However, since EO is extremely reactive, the additional secondary products of DEA and TEA are produced. All three reactions can occur within a short time and are highly exothermic.

(2) Because considerable energy is produced by the above reactions, which increased the temperature of the sample. Then, at high temperature, an exothermic decomposition of EO took place causing the ultimate peaks.

The pressures versus temperature plots in Figure 32 also characterize pressure generation in the EO system. For the most part, the EO/ NH_4OH samples followed the projected curve of ethylene oxide vapor pressure. At about 110 ◦C for 1.0g NH_4OH and 150^{o}C for 0.1g and 0.5g NH_4OH, the pressures from these tests fell away from the projected pressure, presumably because of ethylene oxide consumption. Also reflected in Figure 30 and Figure 32 the mixture pressures were still high despite the cooling period had ended for the scenario of 0.1g and 0.5g NH_4OH. This high measure was due to mixture ignition, following the rupture of the titanium cell with production of less volatile products as well as nitrogen gas, a volatile component, from the containment vessel coming in the sample cell.

Figure 33 shows the time to maximum heat rate which is considerably longer than for the contaminant KOH for a given temperature. In the presence of 0.1g and 0.5g NH_4OH, the mixture gave an explosive decomposition after 227 minutes at near 571°C and 102 minutes at near 530°C.

Very good reproducibility of the experiments was achieved. A summary of some important parameters derived from the data figures above are listed in Table 8. The reported uncertainties are also one standard deviation measured from the experimental replicas.

Table 8 Experimental results of APTAC on EO/NH_4OH mixtures

Contaminant	Φ	T_{on} °C	T_{max} °C	P_{max} psia	dT/dt_{max} °C/min	dP/dt_{max} psi/min	T_{MR} min
0.1g NH_4OH	1.64	158 ± 2	571 ± 9	1749 ± 48	3221 ± 67	3727 ± 82	227 ± 79
0.5g NH_4OH	1.62	59 ± 2	530 ± 4	1763 ± 31	1303 ± 54	12047	102 ± 24
1.0g NH_4OH	1.59	21 ± 1	152 ± 14	390 ± 26	605 ± 30	1139 ± 30	181 ± 19

Compared to the two previous contaminants, the parameters changed in much larger ranges. As can be seen in Table 8, maximum temperature, the maximum pressure, the maximum heat rate, and the maximum pressurization rate decreased as the contaminant weights were increased, which are the less dangerous trends. Only onset temperature tends to more dangerous values. In the presence of only 1.0g NH_4OH, the onset decreased greatly from around 205°C of pure EO to approximately 21°C, followed by the final temperature and pressure of 151°C and 390 psia, which are low values compared to the two other cases. But the onset temperature value of 21°C is low enough to make this scenario extremely hazardous, because EO can react at the ambient condition.

A maximum temperature of over 550^{o}C and a maximum pressure of over 1750 psia can be generated at the smaller amount of contaminant (0.1g and 0.5g) and create dangerous outcomes. Even ignition might have taken place in these tests.

5.5 Ethylene oxide in contact with ethylenediaminetetraacetic acid (EDTA)

This contaminant is the only acid contaminant in this research. Some publications reported that acid has significant effects on EO thermal stability[18]. To evaluate this high impact, the reactivity of 14g pure EO contaminated with various mass of EDTA (0.1g, 0.5g and 1.0g) was examined using the same APTAC operation mode and type of titanium cells. The experimental results are shown in Figure 34 to Figure 39.

Figure 34 depicts the temperature versus time behavior for three different EDTA concentrations. The detected onset temperature increases with the decrease of EDTA concentration and tends towards the value measured for neat ethylene oxide. In the cases of 0.5g and 1.0g EDTA contamination, the maximum temperature and pressure were similar. In the scenario with 0.1g contaminant, however those parameters are much higher (see Figure 34 and Figure 35). Note that during the APTAC cool-down, the pressure in two tests of 0.1g EDTA fell promptly and remained well-below 20 psi. This low pressure was due to of rupture of the titanium cell near exothermic peaks with subsequent bursting of the containment vessel rupture disk causing depressurization to atmospheric pressure. This rupture might have resulted in some inaccuracy on the measured maximum pressures. The mixture final pressure reached over 2200 psia causing the rupture disk to fail. The trend of decrease in the maximum pressure in the sample cell with increases in the EDTA concentration is also observed in Figure 35 and Figure 52 (see page 71).

Figure 36 shows the records of measured heat rate with respect to temperature. The maximum rate of heat generation to 1279^{o}C/min for 0.1g EDTA was much higher than those for 0.5g and 1.0g EDTA. Figure 37 presents the measured pressure rate with respect to temperature. The highest maximum pressure generation rate was 3125 psi/min

for 0.1g EDTA There were no significant differences in those measured rates between the runs in each of the scenarios with 0.5g and 1.0g EDTA.

The final pressure in the sample cell of approximately 60 psi when the sample cooled to 50°C, as shown in Figure 38, is an indication of condensable gas generation in the scenario of 0.5 and 1.0g EDTA. As discussed earlier for 0.1g EDTA, the sample was ejected from the vessel head followed by bursting of the containment vessel rupture disk. As the result, the measured pressure fell to atmospheric level.

Figure 39 shows the time to maximum heat rate at a given temperature. For example, a 14g EO and 0.5g EDTA mixture at approximately 100°C will reach its maximum heat rate in 100 min. The reproducibility of the experiments is clearly observed in these plots.

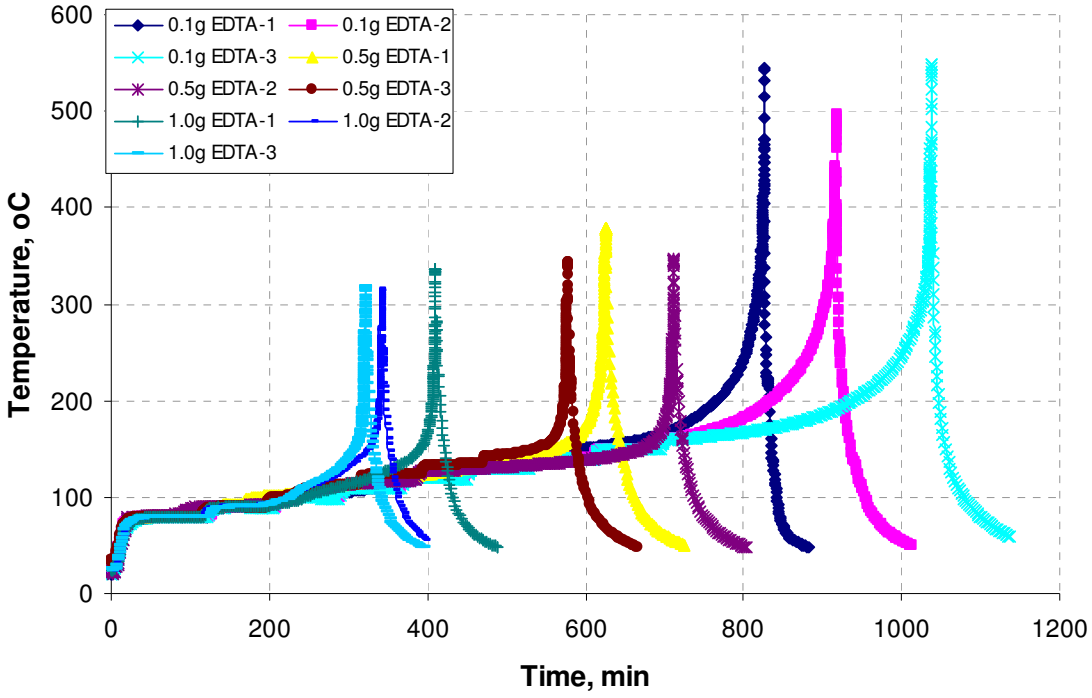

Figure 34 Temperature history profiles of EO/ EDTA samples

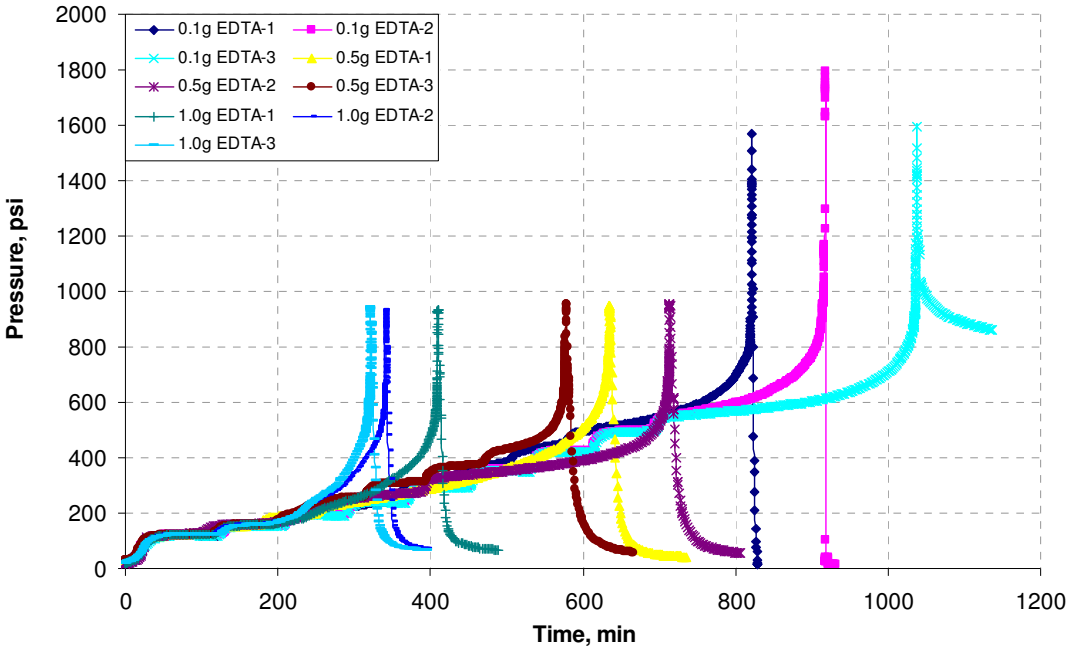

Figure 35 Pressure history profiles of EO/ EDTA samples

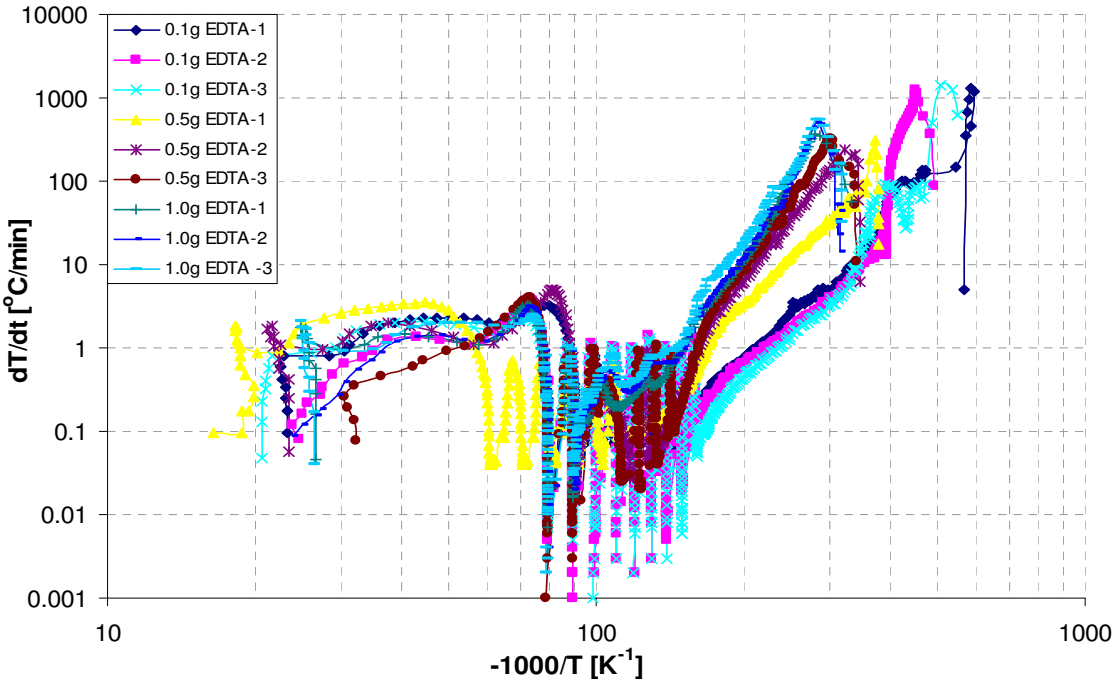

Figure 36 Self-heat rate profiles of EO/ EDTA samples

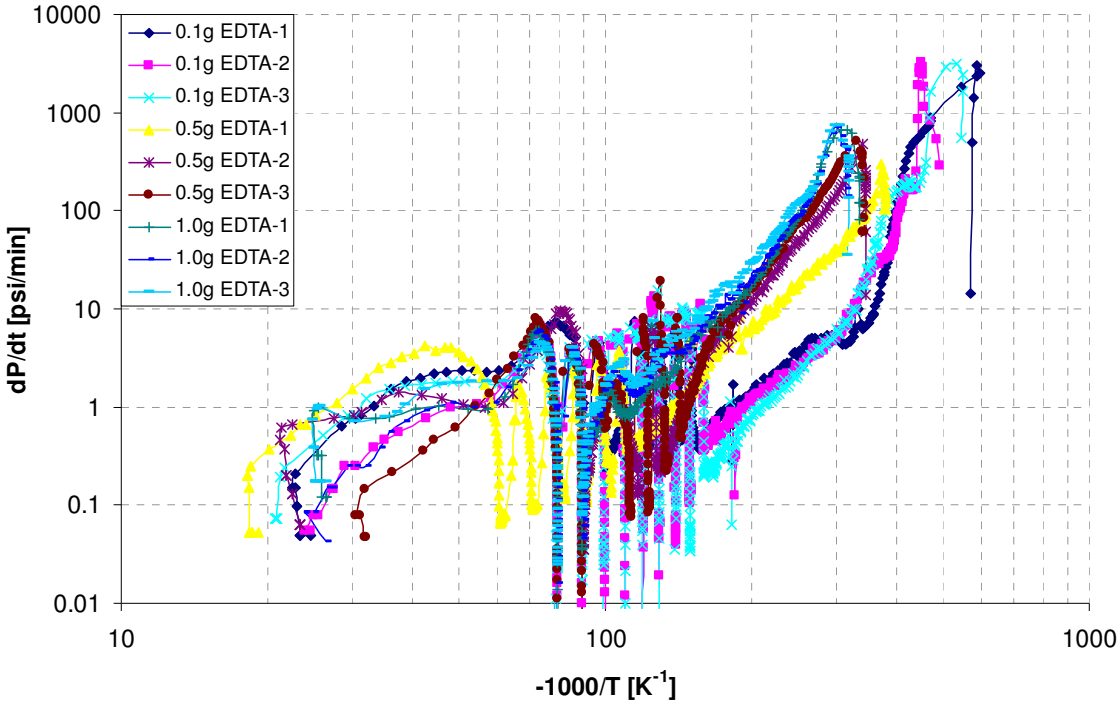

Figure 37 Pressurization rate profiles of EO/ EDTA samples

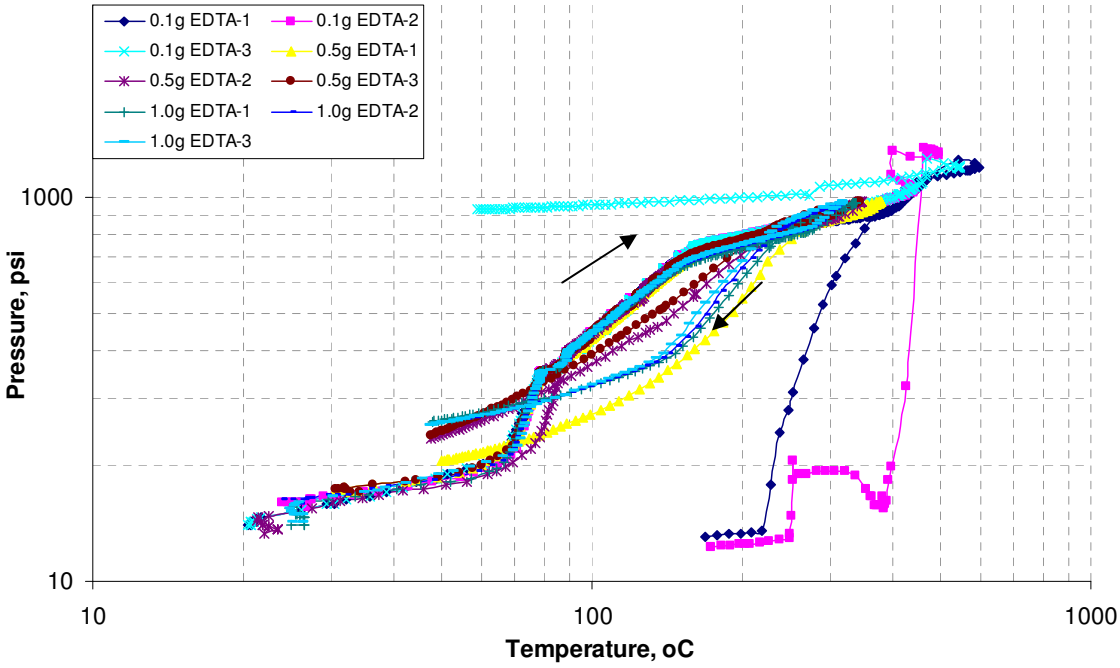

Figure 38 Pressure-temperature profiles of EO/EDTA samples

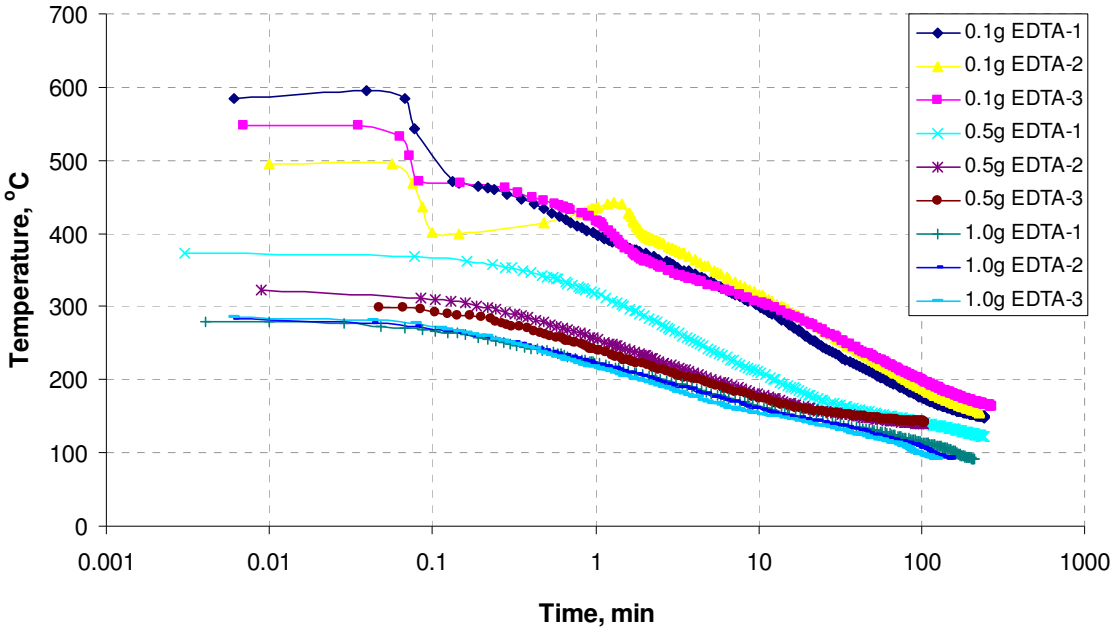

Figure 39 Time-to-maximum profiles of EO/EDTA samples

Table 9 summarizes key parameters. The reported uncertainties are one standard deviation measured from the experimental replicas. Measured dT/dt_{max}, dP/dt_{max} do not show a clear trend. Only onset temperature tends to more hazardous values.

Table 9 Experimental results of APTAC analysis on EO/EDTA mixtures

Contaminant	*Φ*	T_{on} ^oC	T_{max} ^oC	P_{max} *psia*	dT/dt_{max} $^oC/min$	dP/dt_{max} *psi/min*	T_{MR} *min*
0.1g EDTA	1.66	156 ± 7	528 ± 26	1619 ± 56	1279 ± 117	3225 ± 198	245 ± 19
0.5g EDTA	1.64	134 ± 8	356 ± 16	952 ± 3	287 ± 34	434 ± 99	167 ± 32
1.0g EDTA	1.60	92 ± 1	323 ± 9	934 ± 7	475 ± 81	709 ± 28	162 ± 35

5.6 Reactivity comparison of ethylene oxide/contaminants

This section discusses comparisons of the thermal behavior of EO in the presence of four contaminants discussed above. The thermal behavior of pure EO is added in the following tables and figures to make the comparison easier. The scenarios with 0.5g of contaminants are chosen as the reference in most of comparisons.

The temperature versus time behavior of a variety of contaminants in EO is displayed in Figure 40, which clearly shows the effect of different contaminants on the reactivity of EO. Figure 40 indicates that NH_4OH exhibited the highest reactivity of any of the measured samples. The presence of NH_4OH resulted in reduction of the onset temperature significantly, from 205^{o}C of pure EO to around 50^{o}C with generation of the maximum temperatures of over 500^{o}C and maximum pressures of over 1700 psia. Meanwhile, in the presence of contaminant KOH, the onset temperature reduces to 30^{o}C, near room temperature, but its maximum temperature is much lower than that of NH_4OH. On the other hand, the temperature and pressure of contaminant EDTA do not appreciably rise until the sample reaches 130^{o}C. The higher onset temperature of contaminant EDTA reflects the stabilizing influence of the EDTA in EO. In other words, pure EO contaminated by EDTA is safer than with the other contaminants at ambient temperature. Figure 41 displays the same information as Figure 40, except that the curves with pure EO have been added for comparison.

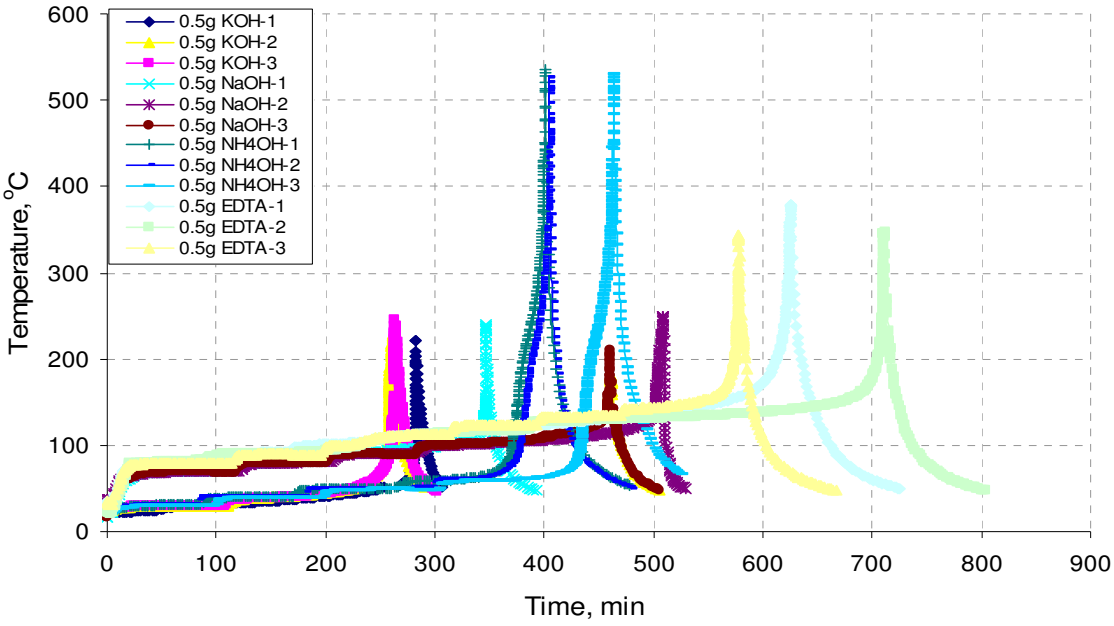

Figure 40 Temperature history profiles of EO/ various contaminants

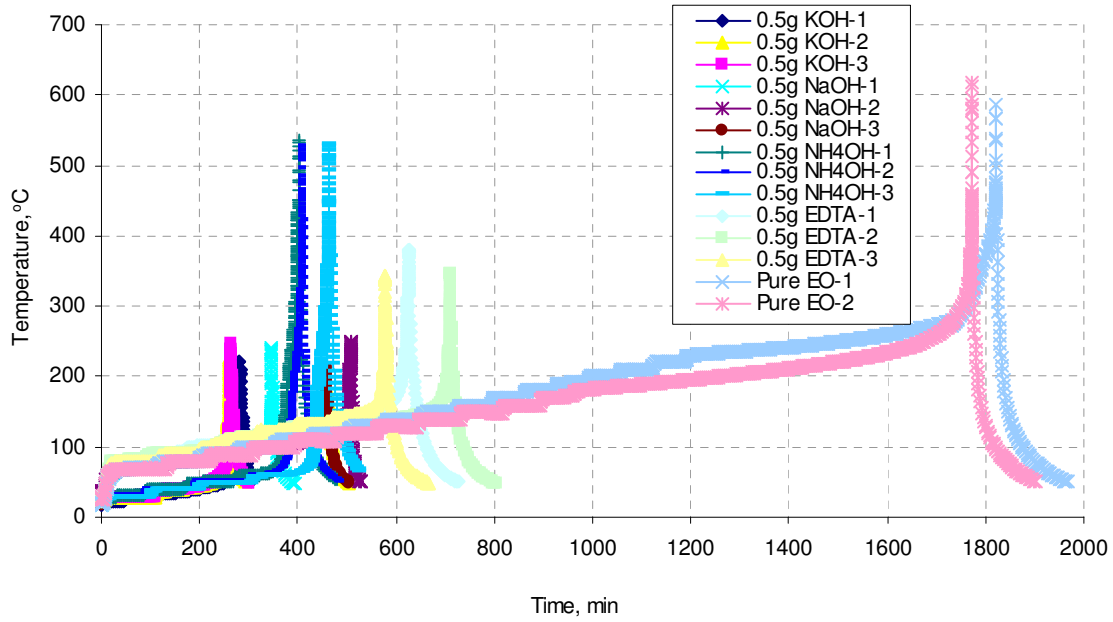

Figure 41 Temperature history profiles of pure EO and EO/ various contaminants

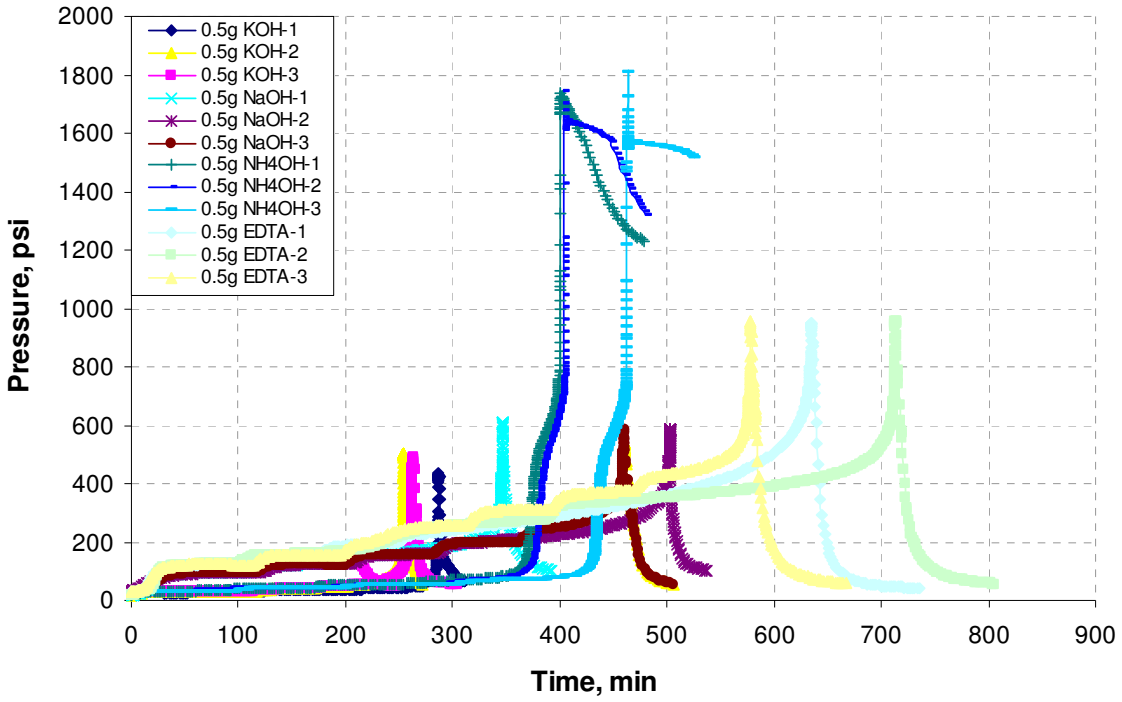

Figure 42 Pressure history profiles of EO/ various contaminants

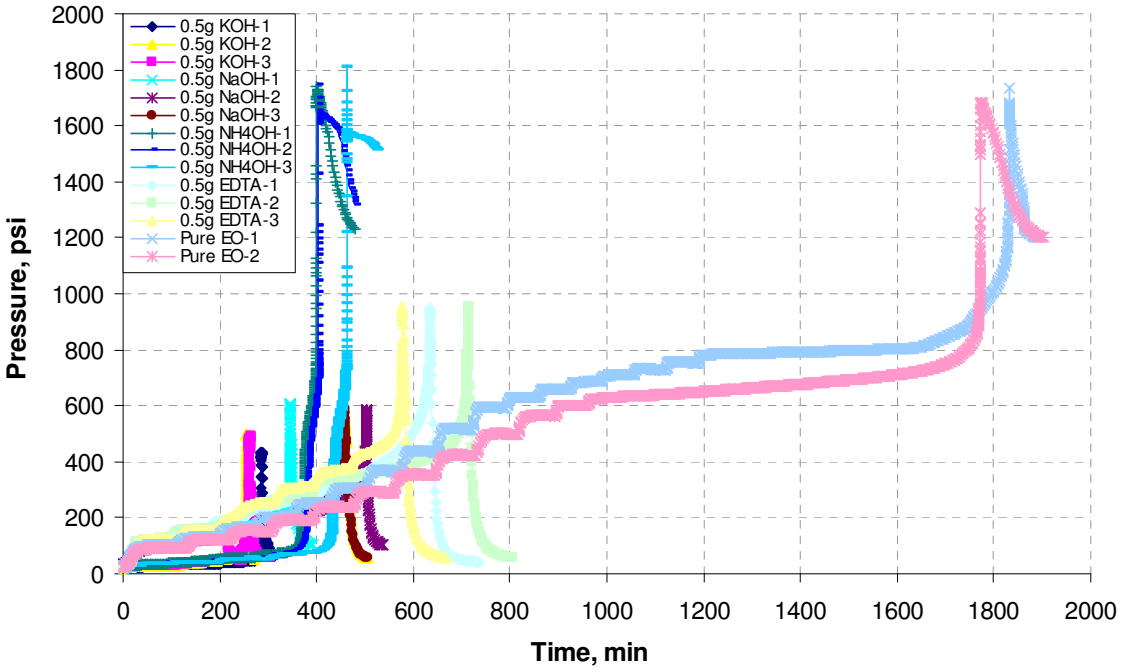

Figure 43 Pressure history profiles of pure EO and EO/ various contaminants

Figure 42 presents pressure versus time plots. For the tests involving KOH and NaOH, the peak pressures did not exceed 650 psi. The pressures in excess of 950 psi were generated for the case with EDTA. For the case with NH_4OH, pressures ultimately exceeded 1700 psi. Again, it seems that NH_4OH is the most reactive contaminant tested due to its low onset temperature and high maximum temperature, pressure, heat rate, and pressure rate. The next most active contaminant from this perspective is the EDTA. The lowest maximum pressure is observed for the KOH (approximately 500 psi). However, the presence of KOH results in the lowest onset temperature, near room temperature. In regard to onset temperature, KOH is more dangerous than NaOH and EDTA. The same pressure versus time curves are displayed in Figure 43 with the pure EO curve added.

The self-heat rate as a function of temperature is illustrated in Figure 44. The same self-heat rate versus temperature curves are displayed in Figure 45 with the pure EO added and the heat-wait-search steps removed for clarify.

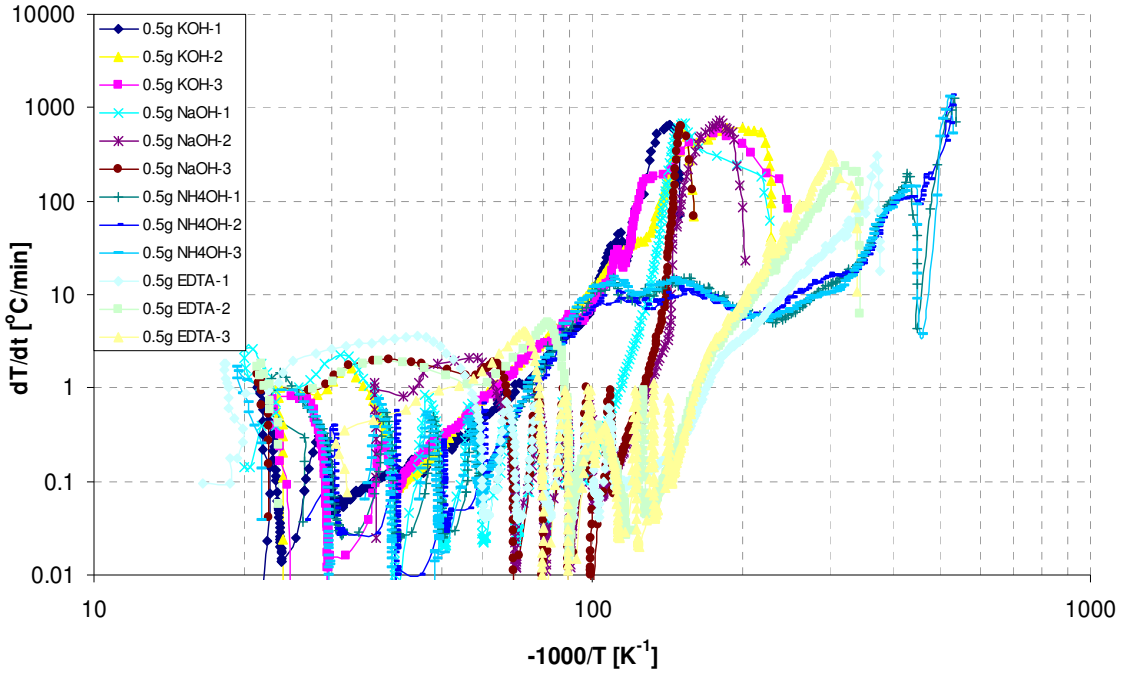

Figure 44 Self-heat rate profiles of EO/ various contaminants

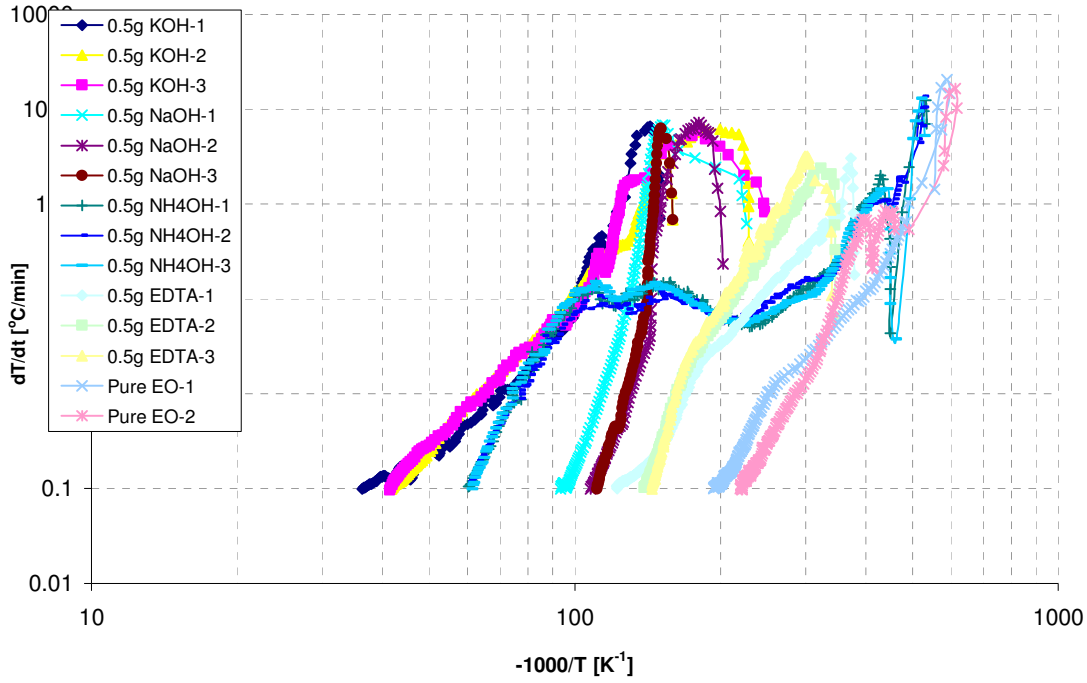

Figure 45 Self-heat rate profiles of pure EO and EO/ various contaminants with the HWS steps removed

As shown in Figure 44 and Figure 45, NH_4OH also exhibits the highest reactivity of any of the sample tested. The NH_4OH had a detectable exotherm at approximately 60°C, increasing to nearly 10°C/min around 100°C. The self-heat rate remained nearly constant until about 280°C and began to accelerate thereafter, giving a self-heat rate up to 150 °C/min at 430°C in the small peak, and then dropping off, until the other stronger exotherm started at 450°C, reaching a bigger peak of roughly 1300 °C/min. With the presence of NH_4OH, the maximum self-heat rates of EO samples were slightly reduced from 1800°C/min (for pure EO) to 1300°C/min, and still much greater than those with the contaminants KOH, NaOH, and EDTA.

The next most active contaminant appears to be KOH. A self-heat rate of roughly 0.1°C/min at near room temperature was observed, but acceleration to over 600°C/min obtained in a short time thereafter. Clearly, the presence of KOH boosts EO

polymerization resulting in EO decomposition to the extent that contact with KOH raises a serious safety concern.

EO in the presence of NaOH appears to show no exothermic activity near room temperature. At 107°C, an exotherm appears that generate a self-heat rate to over 650°C following which the rate then diminishes. The curve for EDTA is parallel to that of the NaOH with an offset of 30-40°C higher temperature but is inclined more at 180°C.

The corresponding pressure rate versus temperature data reported in Figure 47 is the same as in the Figure 46 except for removal of the HWS steps and addition of the curve of pure EO for comparison. The pressure rate curves have the same shapes as the self-heat rate curves. NH_4OH has the greatest pressure rate followed by EDTA, NaOH, and KOH in order.

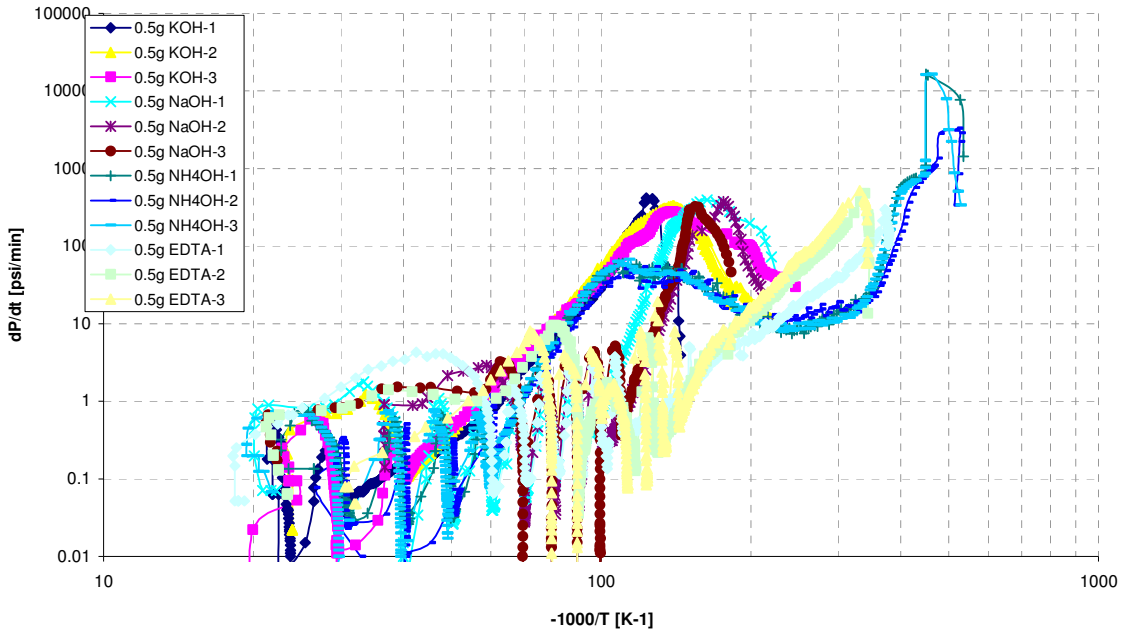

Figure 46 Pressurization rate profiles of EO/ various contaminants

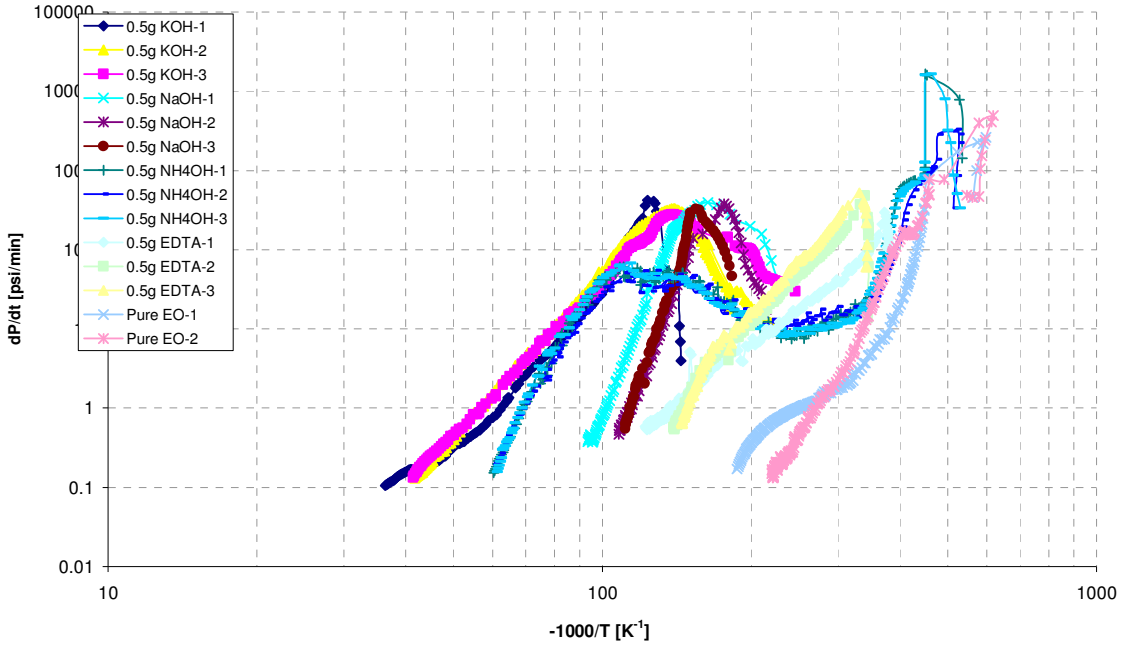

Figure 47 Pressurization rate profiles of pure EO and EO/ various contaminants without the HWS steps

Inspection of the pressure-temperature profiles of Figure 48, by comparison of the heat-up and cool-down portions, reflects the generation of condensable species for the contaminants KOH, NaOH, and EDTA. In the case of the NH_4OH, the final pressure in the sample cell was approximately as high as 1200 psi when the sample cooled to 50^{o}C (see Figure 48) due to the titanium cell rupture. The measured cell pressure was the same as the pressure in the containment vessel which contained the products and nitrogen gas. Hence, the actual maximum pressures creating by the contamination of 0.5g NH_4OH may be higher in the 130ml cell than the maximum pressure reported in this work.

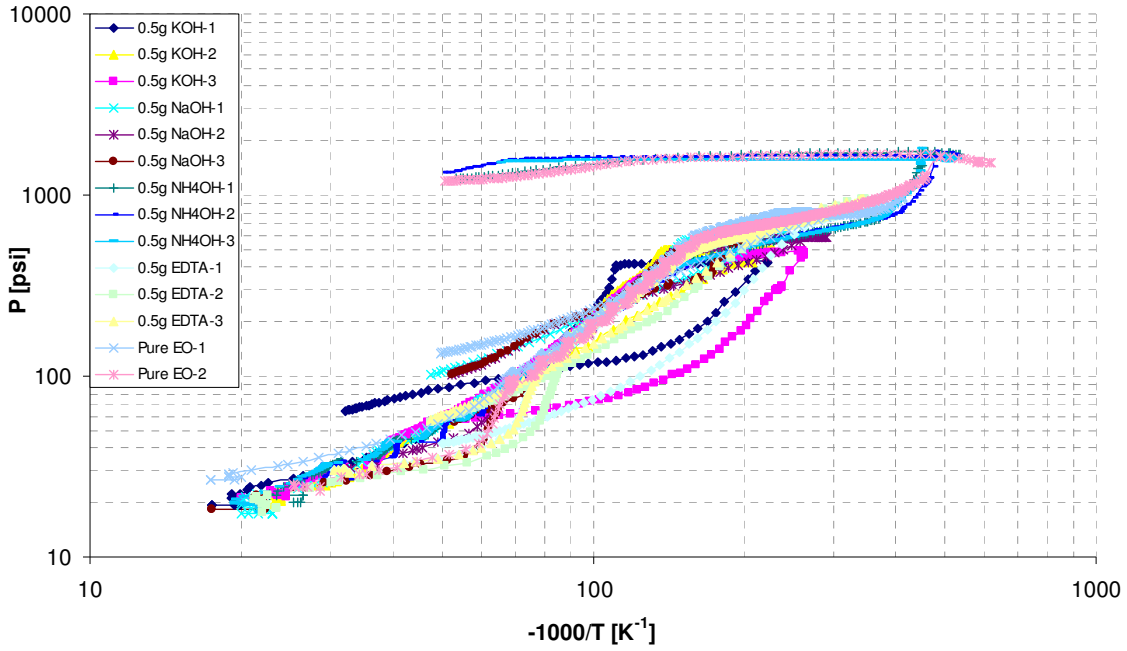

Figure 48 Pressure-temperature profiles of pure EO and EO/ various contaminants

Lastly, the differences in reactivity among species are more clearly illustrated in the time-to-maximum rate plot of Figure 49. In the presence of KOH, at near ambient temperature, less than 70 minutes is needed for the reaction rate to reach its maximum; by 80-100^{o}C, the time is only about 1 minute to reach the temperature of approximately 180^{o}C and the maximum rate. From this perspective, it seems that the KOH/EO mixture has a somewhat higher reactivity than in NaOH contamination and a much higher reactivity than the EDTA/EO mixture. Although the time required to reach the overall maximum for NH_4OH (around 530^{o}C) is approximately 100 minutes, longer than that for KOH, it is still considered the most reactive contaminant. As can be seen from Figure 49, by 90^{o}C, the time is only about 30 minutes to reach 530^{o}C, almost 3 times greater than that of KOH.

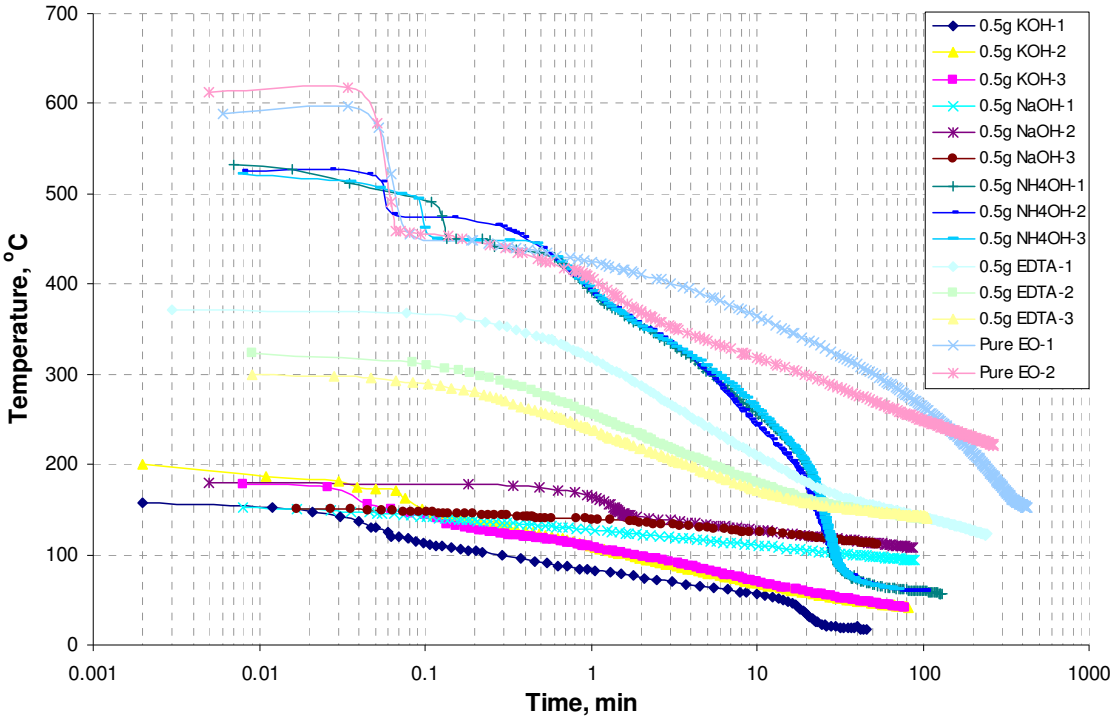

Figure 49 Time-to-maximum profiles of pure EO and EO/ various contaminants

Table 10 presents a compilation of measured parameters which have been discussed and shown in the previous paragraphs.

Table 10 Important parameters reflected the reactivity of EO in the presence of contaminants

Contaminant	*Φ*	T_{on} ^oC	T_{max} ^oC	P_{max} *psia*	dT/dt_{max} $^oC/min$	dP/dt_{max} *psia/min*	T_{MR} *Min*
0.5g KOH	1.62	40 ± 2	231 ± 10	475 ± 28	620 ± 30	342 ± 58	69 ± 16
0.5g NaOH	1.62	108 ± 3	233 ± 16	594 ± 11	679 ± 40	365 ± 29	62 ± 2
0.5g NH_4OH	1.62	59 ± 2	530 ± 4	1763 ± 31	1303 ± 54	12047	102 ± 24
0.5g EDTA	1.64	134 ± 8	356 ± 16	952 ± 3	287 ± 34	434 ± 99	150 ± 65
(None)	1.64	205 ± 16	600 ± 13	1709 ± 27	1694 ± 49	3859 ± 75	296 ± 27

The onset temperature is the most important parameter to evaluate the contamination effects on EO thermal stability. Figure 50 compare the onset temperatures of different contaminants and different contaminant concentration to illustrate the impact of contaminants concentration on the detected exothermic onset temperatures more clearly. These T_o values are the average values from the test results. The detected onset temperature increases as the contaminant mass is decreased and tends towards the value measured for pure EO. This figure clearly shows that the stability of EO is strongly affected by the KOH. The onset temperature of pure EO is reduced remarkably even at a small amount of KOH (0.1g). The thermal onset temperatures obtained by the APTAC with various investigated NaOH, KOH, and EDTA concentrations change slightly, but those with NH_4OH change dramatically.

Figure 50 also shows that the behavior of the NaOH appears to parallel that of the KOH except for being displaced to a 60-70^oC higher onset temperature. This phenomenon is interesting because KOH and NaOH have similar structures and properties, but their effects on EO are quite different.

The relationships between the mass of various contaminants and the T_{max}, P_{max}, dT/dt_{max}, dP/dt_{max}, and T_{MR} values, the average values of some tests, are shown from Figure 51 to Figure 55. In general, the maximum temperature, maximum pressure, maximum heat rise rate, maximum pressurization rate and time-to-maximum rate decrease with the increase of the contaminant mass except for the unclear trends of the maximum self-heat rate and the maximum pressure rise rate of the contaminant EDTA.

In short, as increasing contaminant concentration, the onset temperatures, maximum temperatures, maximum pressures, maximum self-heat rates, maximum pressure rise rate, and time-to-maximum rates changed slightly for contaminant KOH, significantly for NH_4OH and EDTA, but almost similar for NaOH. For contaminant KOH, the T_o, dT/dt_{max}, dP/dt_{max}, T_{MR} changed to more dangerous values (T_o, T_{MR}: reduce; dT/dt_{max}, dP/dt_{max}: increase). While, for each of NaOH, NH_4OH, and EDTA, only T_o, T_{MR} tend to more dangerous values.

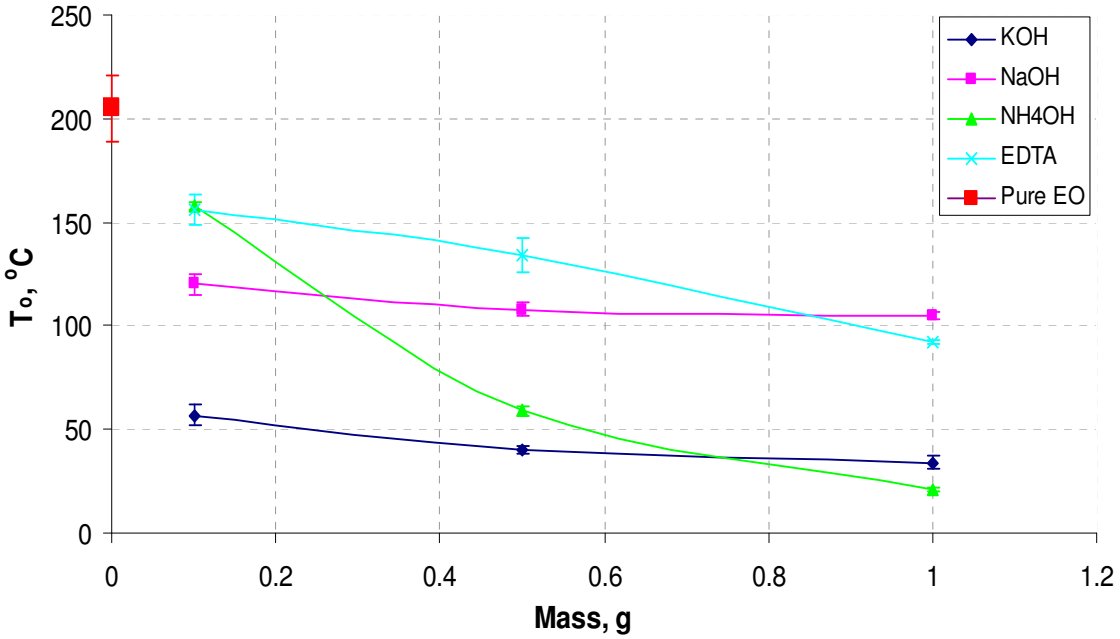

Figure 50 Onset temperature-mass of contaminants profiles

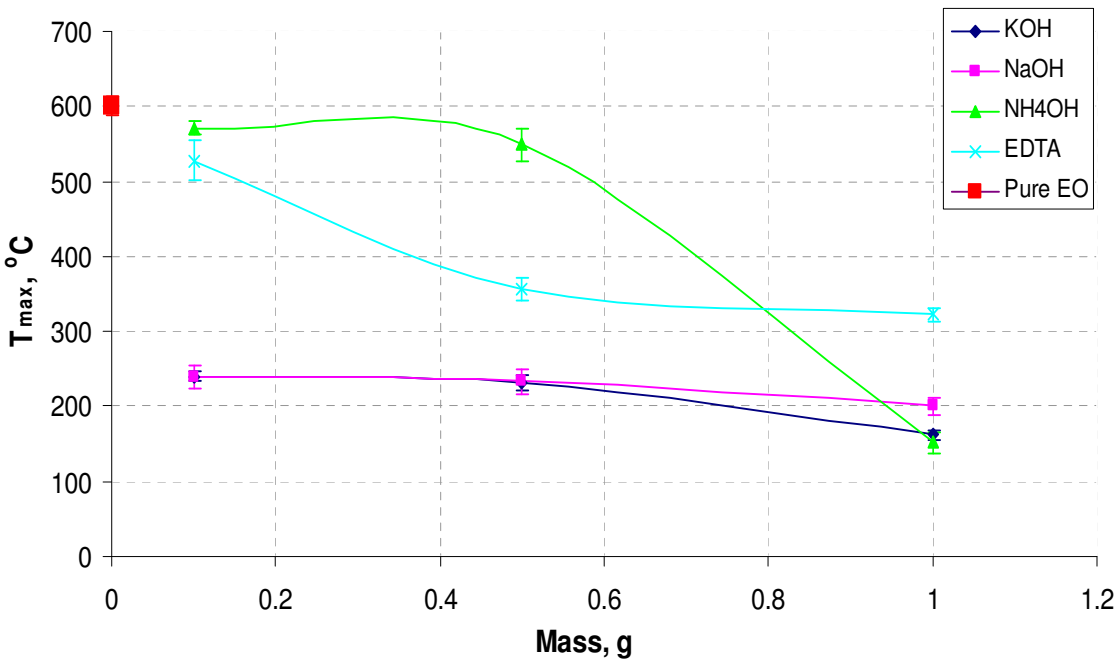

Figure 51 Maximum temperature-mass of contaminants profiles

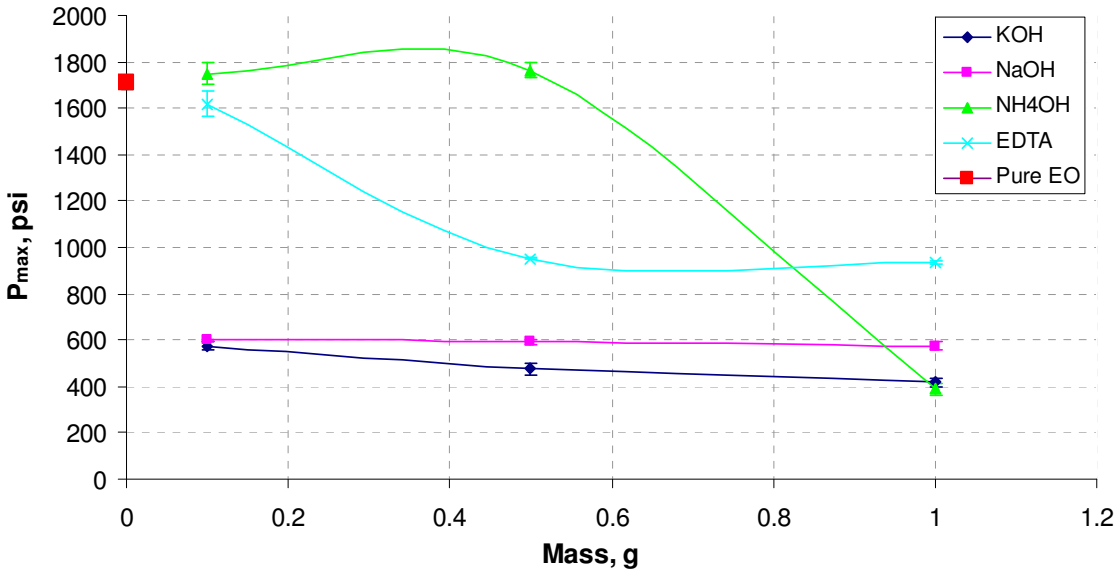

Figure 52 Maximum pressure-mass of contaminants profiles

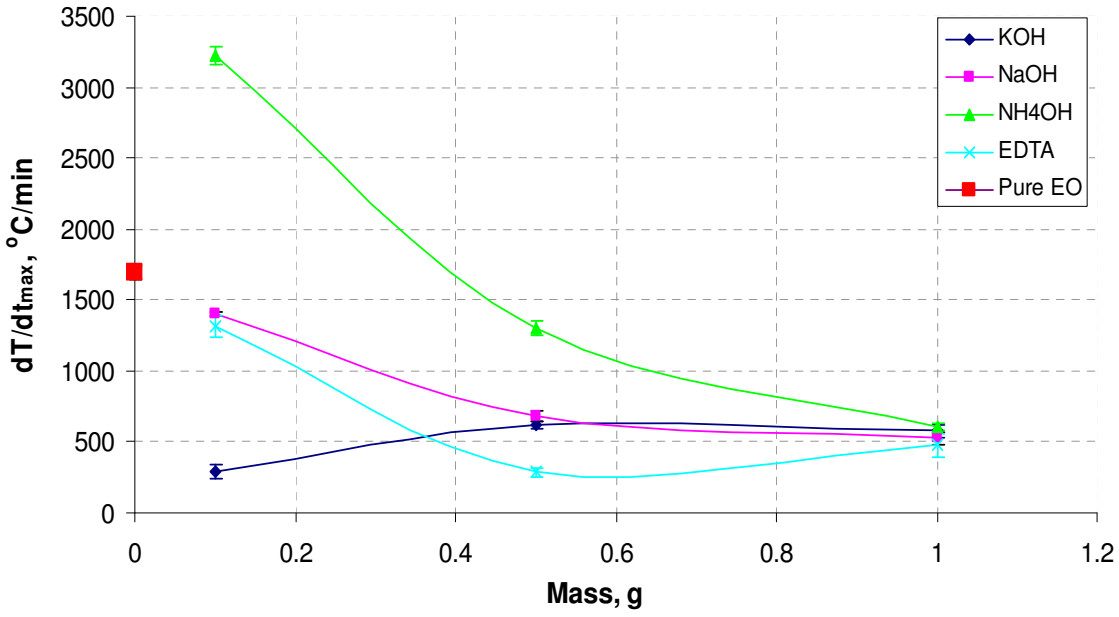

Figure 53 Maximum heat rate-mass of contaminants profiles

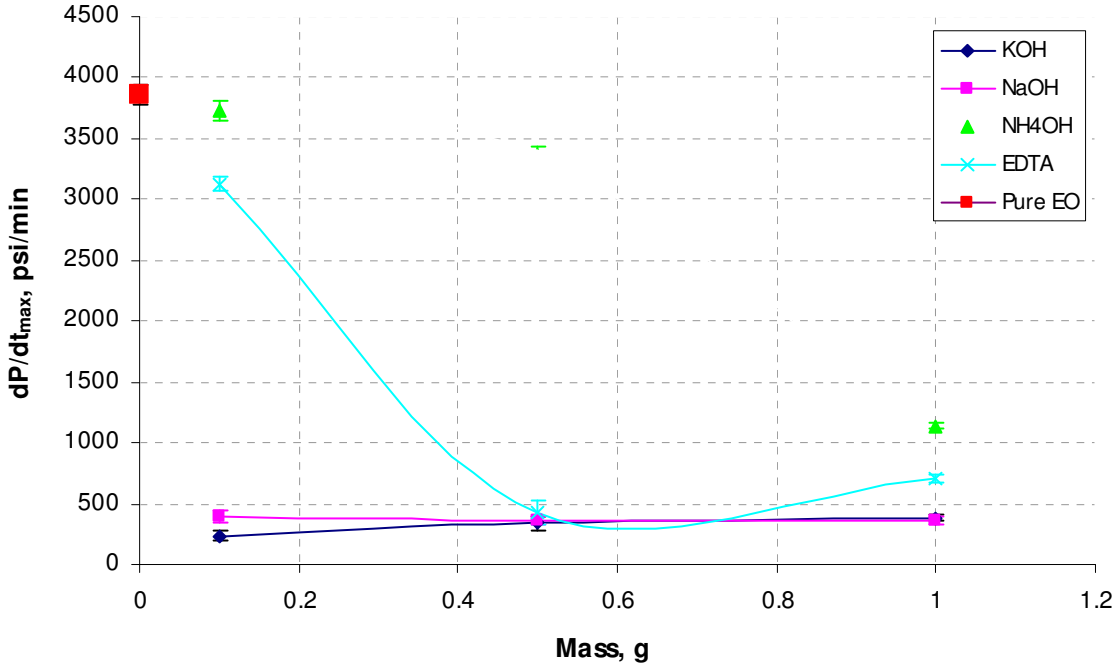

Figure 54 Maximum pressurization rate-mass of contaminant profiles

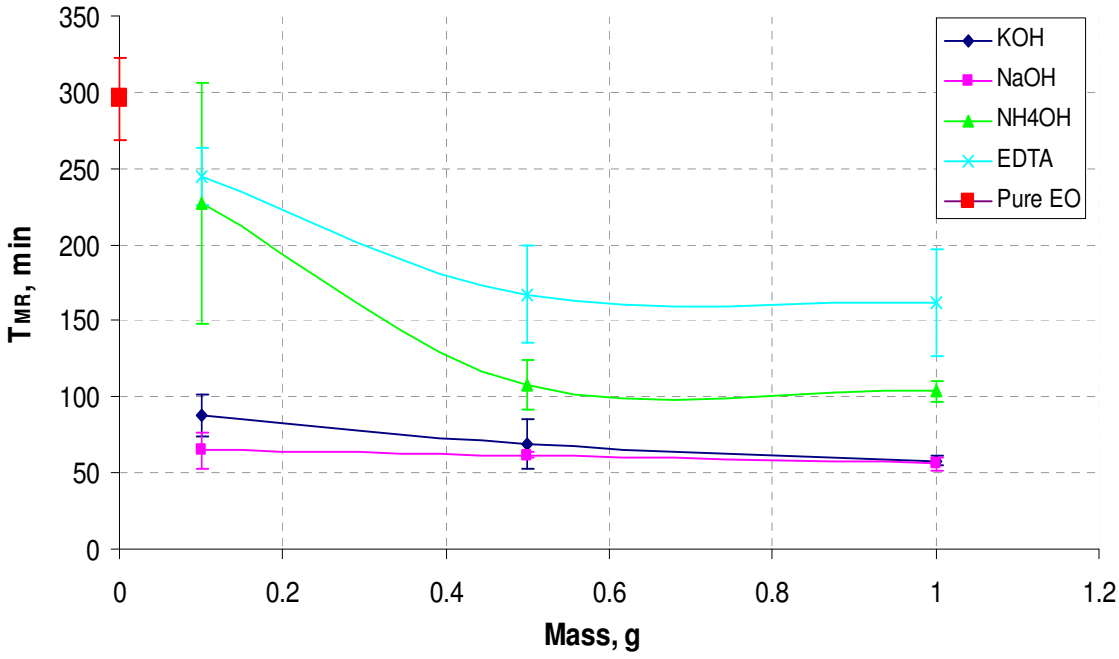

Figure 55 Time-to-maximum and mass of contaminants profiles

CHAPTER VI

CONCLUSIONS AND RECOMMENDATIONS

6.1 Conclusions

Evaluation of the reactivity of ethylene oxide (EO) in contact with various contaminants has been performed via measurements using an Automatic Pressure Tracking Adiabatic Calorimeter (APTAC). Four investigated contaminants, which can contact EO in industrial processes, are anhydrous potassium hydroxide (KOH), anhydrous sodium hydroxide (NaOH), ammonia aqueous solution (NH_4OH), and ethylene diamine tetraacetic acid (EDTA). Various small amounts (0.1 gram, 0.5 gram, and 1.0 gram) of these chemical compounds were mixed with 14 gram EO in an automatic pressure tracking adiabatic calorimeter and heated to measure the exotherm reaction behavior of EO.

The 14 gram of pure EO required about 205^{o}C to initiate runaway reaction under adiabatic conditions and produced a maximum temperature of about 600^{o}C and pressure of approximately 1710 psia. The tested contaminants affected measured values of these parameters. All of the contaminants greatly exhibited catalytic effects on the reactivity of EO and caused to reduce in the runaway reaction threshold temperature, which increases the hazard of EO.

In the studied range of contaminant concentrations, the onset temperatures, maximum temperature rates, maximum pressure rates and time to maximum heat rates changed to more dangerous values when the amount of KOH increased. With each of NaOH, NH_4OH, and EDTA, the contaminated EO underwent exotherm reactions at more hazardous (lower) values of onset temperatures and time to maximum heat rates.

At the same tested concentrations, the EO reactivity was compared among contaminants. Although the contaminants all lowered the onset temperature of EO, they showed different affecting levels. In an amount of 1g, NaOH and EDTA reduced the onset temperature to around 100^{o}C while KOH and NH_4OH decreased it to a room temperature, which is extremely dangerous. Among the investigated contaminants, the presence of NH_4OH with a sufficient concentration has the highest impact on the maximum temperature, pressure, heat rate, and pressurization rate of contaminated EO. By 59^{o}C, 0.5g NH_4OH (~3.5 % wt.) gave an explosive decomposition after 102 minutes at near 530^{o}C. But in general, KOH is the most hazardous contaminant, because it can make an exotherm start at room temperature even with a low concentration, which is more likely to occur in industry. The following relative reactivity of contamination is suggested: NH_4OH > KOH > NaOH > EDTA. Serious safety concerns should be made to avoid these contaminations of EO.

6.2 Recommendations for future work

To be most of use, the thermokinetics of the reactions of EO with KOH, NaOH, NH_4OH, and EDTA need to be determined. At present, this research investigates three scenarios of concentrations for each contaminant and the analysis appears to be complicated by the rapid change in the thermodynamic properties of EO in the critical region. Additional experiments over wider ranges of phi-factor and EO mass fraction as well as product identification should be made to gain enough experiment data for a thorough kinetics understanding and development of kinetic models for these reactions.

Then, a larger number of experimental data, the mechanism and kinetics model for these exothermic reactions can be used to develop simulation models to reproduce measured data from APTAC and predict scaled-up onset temperature, time to maximum rate, and maximum pressure for ranges of EO volume, concentration, and operation conditions. That future work can aid safety-related decisions regarding processing, storaging and handling, stable conditions, emergency relief system, and incident investigations. In addition, it will be very valuable for inherently safer process safety designs.

LITERATURE CITED

1. ARIP. Accidental release information program database. *United State Environmental Protection Agency.* September 1994.

2. HSEES. Hazardous substances emergence events surveillance database. *The Agency for Toxic Substances and Disease Registry.* 1996-2001.

3. Viera G, Simpson LL, Ream BC. Lessons learned from the ethylene oxide explosion at Seadrift, Texas. *Chem. Eng. Prog*. 1993; 89: 66-75.

4. Report on carcinogens, eleventh edition. *http://ntp.niehs.nih.gov/ntp/roc/toc11.html.* Accessed January 24, 2008

5. Preventing worker injuries and deaths from explosions in industrial ethylene oxide sterilization facilities. *http://www.cdc.gov/niosh/docs/2007-164/.* Accessed February 04, 2008.

6. Buckles C, Chipman P, Cubillas M, Lakin M, Slezak D, Townsend D, Vogel K, Wagner M. Ethylene oxide user's guide, second edition. *http://www.ethyleneoxide.com.* 1999. Accessed August 07, 2007.

7. Dever JP, George KF, Hoffman WC, and Soo H. Ethylene oxide. *Kirk-Othmer Encyclopedia of Chemical Ttechnology, fourth edition*. 1994; 9: 915-959.

8. Vanderwater RG. Case history of an ethylene oxide tank car explosion. *Chemical Engineering Progress*. 1989; 85:16-20.

9. Burridge E. Ethylene oxide. *European Chemical News*. 2005; 83: 2157.

10. Virtanen POI. Kinetics of the hydrolysis reactions of ethylene oxide. *Ann. Academiae Scientiarum Fenticae.* 1963; A: 9-89.

11. Woodward J, Wesevich JW, Thomas JK, and Baker QA. Analysis of ethylene oxide gas house explosion. *Process Safety Progress*. June 2007; 26(2): 150-154.

12. Kletz TA. Fires and explosions of hydrocarbon oxidation plants. *Plant/Operations Progress*. 1988; 7(4): 226-230.

13. Bretherick L, Urben PG. *Bretherick's handbook of reactive chemical hazards.* Butterworth-Heinemann, fifth edition. 1995; 272-276.

14. Troyan JE, and LeVine RY. Ethylene oxide explosion at Doe Run. *AlChE Loss Prevention*. 1968; 2: 125-130.

15. Gustin JL. Safety of ethoxylation reactions. *Hazards XV—the process, its safety and the environment.* 2000; I. Chem. E. Symp. Ser. 147: 251-263.

16. Britton LG. Thermal stability and deflagration of ethylene oxide. *Plant/Operations Progress*. 1990; 9(2): 75-86.

17. Levin ME. The reactivity of ethylene oxide in contact with iron oxide fines as measured by adiabatic calorimetry. *Journal of Hazardous Materials*. 2003; 104: 227-245.

18. Melhem GA, Levin ME, Fisher HG, Chippelt S, Singh SK, and Chipman PL. Kinetics of the reactions of ethylene oxide with water and ethylene glycols. *Process Safety Program*. 2001; 20(4): 231-246.

19. Freeder S, Snee TJ. Alkali-catalysed polymerization of ethylene oxide and propylene oxide- hazard evaluation using accelerating rate calorimetry. *J. Loss Prev. Process*. 1988; 1: 164-168.

20. Cisneros, L.O., Adiabatic calorimetric studies of hydroxylamine compounds. *PhD Dissertation, Texas A & M University, College Station, Texas*, August 2002.

21. Legget D, Singh J, Process improvements from incident data. *Process Safety Progress*. 2000; 19: 13-18.

22. Granville R, Wallace D. Accelerating rate calorimetry: instrumentation and application. *Proceedings of the International Symposium on Runaway Reactions and Pressure Relief Design*. Boston, MA. 1995; 10-22.

23 Chippett S, Ralbovsky P, Granville R. The APTAC: a high pressure, low thermal inertia, adiabatic calorimeter. *Proceedings of the Internatinal Symposium on Runaway Reaction, Pressure Relief Design and Effluent Handling*. 1998; 81-108.

24. Cisneros L, Rogers WJ, Mannan SM. Adiabatic calorimetric decomposition studies of 50 wt.% hydroxylamine/water. *Journal of Hazardous Materials*, 2001; 82: 13-24.

25. Sempere J, Nomen R, Serra R, Cardillo P. Thermal hazard assessment using closed cell adiabatic calorimetry. *Journal of Loss Prevention Process Industry*, 1997; 10: 55-62.

26. Gonzales N, Levin ME. Solvent effects on di-tert butyl peroxide decomposition. *Mary Kay O'Connor Process Safety Center Symposium Proceedings*. College Station. October 23-24, 2006.

27. Aldeeb AA. Systematic approach for chemical reactivity evaluation. *PhD Dissertation, Texas A & M University, College Station, Texas*. Dec 2003.

28. Wilcock E, Rogers R. A review of the phi factor during runaway conditions. *Journal of Loss Prevention in the Process Industries*. 1997; 10: 289-302.

29. Gonzales N, Levin ME, Zimmerman LW. The reactivity of sodium borohydride with various species as characterized by adiabatic calorimetry. *Journal of Hazardous Materials*. 2007; 142: 639-646.

30. Efunda. http://www.efunda.com/materials/elements/HC_Table.cfm?Element_ID=Ti. Accessed March 20, 2008

31. Serio M, Tesser R, Felippone F, Santacesaria E. Ethylene oxide solubility and ethoxylation kinetics in the synthesis of non ionic surfactants. *Industrial Engineering Chemical Research*. 1995; 34(11): 4092-4098.

32. Patent storm. http://www.patentstorm.us/patents/5545757-description.html: Production of ethanolamines. Accessed March 20, 2008.

VITA

Name: Linh T.T. Dinh

Address: Department of Chemical Engineering, Texas A&M University
3122 TAMU, College Station, TX 77840

Email Address: dinh@tamu.edu

Education: B.S., Chemical Engineering, Ho Chi Minh City University of Technology, 2002
M.S., Chemical Engineering, Texas A&M University, 2008